sustainability

MDPI

Article

Promoting Sustainability: Collaborative Governance Pathways for Virtual Water Interactions and Environmental Emissions

Jiawen Yu [1,2,*], Shengyang Pu [3,4,*], Hui Cheng [5], Cai Ren [6], Xiaoying Lai [7] and Aihua Long [7]

1 Zhejiang Ecological Civilization Academy, Anji 313300, China
2 School of Public Affairs, Zhejiang University, Hangzhou 310058, China
3 Xinjiang Institute of Water Resources and Hydropower Research, Urumqi 830049, China
4 Nanjing Hydraulic Research Institute, Nanjing 210029, China
5 Yellow River Engineering Consulting Co., Ltd., Zhengzhou 450003, China; slchengh@163.com
6 College of Water Conservancy & Architectural Engineering, Shihezi University, Shihezi 832000, China; cyrus1837@163.com
7 College of Management and Economics, Tianjin University, Tianjin 300072, China; xiaoying.lai@tju.edu.cn (X.L.); aihua_long@tju.edu.cn (A.L.)
* Correspondence: yujiawen_415@163.com (J.Y.); xjskypsy@163.com (S.P.)

Abstract: This study explores the water consumption and greenhouse gas (GHG) emissions in the Yarkand River Basin, focusing on their dynamic interactions across industrial sectors. Utilizing environmental input–output analysis (IOA), the CROPWAT model, and life cycle assessment (LCA), we quantified the historical evolution of physical and virtual water cycles in relation to the water–carbon nexus. Our findings reveal that the planting industry, particularly the production of export-oriented, water-intensive crops like cotton, significantly contributes to both blue and green water consumption, exacerbating regional water scarcity. The persistent external market demand drives this over-extraction, further strained by the basin's limited water retention capabilities. Although advancements have been made in reducing the per-unit water footprint of crops, total water consumption continues to rise due to agricultural expansion, intensifying pressure on blue water resources. Additionally, agricultural GHG emissions have surged, driven by increased electricity consumption, heavy fertilizer use, and escalating soil N_2O emissions. In light of these challenges, our research underscores the critical need for integrated resource management strategies that align with sustainable development goals. By promoting efficient water allocation within the agricultural sector and diversifying crop structures downstream, we can enhance ecosystem resilience and reduce environmental degradation. Furthermore, the advancement of value-added agricultural processing and the implementation of innovative water conservation technologies are essential for fostering economic sustainability. These strategies not only mitigate the environmental impacts associated with agricultural practices but also strengthen the region's adaptive capacity in the face of climate change and fluctuating market demands. Our findings contribute to the broader discourse on sustainable agricultural practices, emphasizing the interconnectedness of water management, climate resilience, and economic viability in arid regions.

Keywords: collaborative governance; water footprint; GHG emissions; industry sustainability; Yarkand River Basin

check for updates

Citation: Yu, J.; Pu, S.; Cheng, H.; Ren, C.; Lai, X.; Long, A. Promoting Sustainability: Collaborative Governance Pathways for Virtual Water Interactions and Environmental Emissions. *Sustainability* **2024**, *16*, 9309. https://doi.org/10.3390/su16219309

Academic Editors: Sandra Mourato and Cristina Andrade

Received: 26 September 2024
Revised: 21 October 2024
Accepted: 24 October 2024
Published: 26 October 2024

Copyright: © 2024 by the authors. Licensee MDPI, Basel, Switzerland. This article is an open access article distributed under the terms and conditions of the Creative Commons Attribution (CC BY) license (https://creativecommons.org/licenses/by/4.0/).

1. Introduction

The increasing competition for global resources, fueled by rapid population growth and environmental degradation, presents a critical challenge for humanity [1]. By 2050, global demand for freshwater, food, and energy is projected to exceed that of 2020 by over 50%, underscoring the pivotal role these resources play in sustaining human life and fostering regional stability [2]. Agriculture, responsible for 70% of global water use and nearly 30% of global energy consumption, exemplifies the complex interconnections between water use, crop production, and environmental emissions [3–5]. These intertwined dynamics

highlight the urgent need for policymakers to adopt integrated resource management approaches, moving beyond fragmented strategies that often lack coordination. Watersheds, as natural and socio-economic boundaries, provide a comprehensive perspective on the interactions between ecosystems and human activities. This has led to a growing focus on aligning basin-scale resource use with sustainable environmental governance, thereby bridging gaps between ecological and political boundaries [6].

In this context, environmental accounting methods, such as input–output analysis, environmental footprint accounting, and life cycle assessment, play a crucial role in quantifying the resource demands and impacts of human activities [7]. The input–output model, initially based on the classical Leontief framework, has been extended to include resource considerations in economic analysis [8]. Scholars have effectively employed this model to assess resource consumption across industries, revealing insights into regional resource efficiency and trade dynamics [9,10]. Recent advancements in data availability and computational capabilities have enhanced the application of these models to analyze complex systems at finer scales [11,12]. By integrating "top-down" models with "bottom-up" approaches, such as environmental footprint analyses, researchers have gained deeper insights into resource demands across supply chains [13,14]. When integrated with life cycle assessment, these methods allow for the quantification of resource use and environmental pressures across various stages of a product's lifecycle, offering a more comprehensive understanding of environmental impacts [15]. For instance, research indicates that substituting fossil fuels with alternative energy sources may reduce carbon footprints while increasing water footprints, highlighting the necessity for policymakers to collaborate with local stakeholders to address potential tradeoffs [16]. While individual environmental footprint assessments—focusing on a single metric like water or carbon—offer valuable insights, integrated analyses of multiple footprints provide a deeper understanding of the tradeoffs and synergies within systems or industries [17,18]. Systematizing the relationship between resource flows and environmental footprints across sectors can provide a practical coordination approach to guide refined management practices [19]. Such accounting must be conducted at all stages of the industrial supply chain to ensure informed decision making. Scholars have also examined the environmental footprints of agricultural products from a consumption perspective, assessing how agricultural demand impacts various environmental dimensions across different spatial scales [20]. This reverse perspective—analyzing how critical resources and environmental emissions shape industrial production and the virtual interactions of resources across sectors—is crucial to developing collaborative governance strategies for arid inland regions that seek to balance economic development and environmental protection.

This study focuses on the Yarkand River Basin in China's arid inland region, a prime example of the challenges faced in managing scarce water resources within fragile ecosystems [21]. This study examines the physical water and virtual water dynamics in the region over the past 25 years, with a particular focus on blue water and green water in key industries. Virtual water refers to the volume of freshwater utilized in the production of consumer goods, which can be transported and traded [22]. Blue water encompasses the surface water and groundwater available for human use, including irrigation and drinking purposes. Green water is the precipitation stored in the soil that plants use for growth, representing the moisture supplied in the form of rainfall [23]. By systematically analyzing the interaction processes and transformation patterns of resources, this study aims to explore the evolution of the environmental footprint associated with industrial activities. We specifically focus on identifying key strategies for balancing water resource consumption and greenhouse gas emissions in critical industries within the Yarkand River Basin. To achieve this, we employ a comprehensive framework that integrates environmental input–output analysis (IOA) with bottom-up methodologies, such as the CROPWAT model and life cycle assessment (LCA). This combination allows us to provide a holistic understanding of the actual consumption and emissions of water and carbon resources. Our previous research has validated the collaborative applications of these methods, as demonstrated in our

published works on inter-sectoral virtual water reallocation and sustainable intensification levels in dryland agriculture [24,25]. This approach fills a significant gap in the existing literature on resource and environmental management in the Yarkand River Basin, offering novel insights into synergistic governance strategies that balance industrial growth with sustainable ecosystem development. Through this work, we aim to elucidate the complex interactions between human activities, natural resource use, and environmental impacts in arid inland regions.

2. Methodology

2.1. Study Area

The study area is the Yarkand River Basin (YRB, 34°50′–40°31′ N, 74°28′–80°54′ E), with a total land area of 85,800 km^2. Located in the heart of the Eurasian continent, the basin is administratively part of China's Xinjiang Uygur Autonomous Region, encompassing the counties of Yecheng (YC), Shache (SC), Zepu (ZP), Maigaiti (MT), Bachu (BC), and Tashkurgan (TG). The region has a warm temperate, continental, arid climate characterized by an average annual temperature of 11.4–11.8 °C, low precipitation (less than 110 mm annually), and high evaporation rates, ranging between 2109 and 2480 mm per year. These climatic conditions provide a solid foundation for agricultural development, with cotton and fruits as the primary crops. According to the Statistic Bureau of Xinjiang Uygur Autonomous Region (https://tjj.xinjiang.gov.cn/, accessed on 25 September 2024, the same below), by the end of 2015, the total population of the study area was approximately 2.28 million. Urbanization remains relatively low, with an urbanization rate of only 20.5%, significantly below the regional average (47.2%) and the national average (56.1%). The region's gross domestic product (GDP) was 34.092 billion CNY, with the primary, secondary, and tertiary industries contributing 40.7, 21.7, and 37.6%, respectively. The per capita GDP stood at 14,900 CNY. In 2015, the total water supply in the study area reached 6.085 billion m^3, with surface water and groundwater accounting for 80.8 and 19.2% of the total, respectively. The total water consumption for the same year was 6.335 billion m^3, of which agricultural water use dominated, accounting for 98.4% (6.234 billion m^3). Industrial, domestic, and ecological water use amounted to less than 100 million m^3. Between 1990 and 2015, the average annual crop sown area was 4064.34 km^2, and the average annual cultivated land area was 2785.88 km^2. By 2015, the actual irrigated area reached 5957.73 km^2, with farmland irrigation covering 5348.00 km^2. Fossil fuel consumption in the region in 2015 was 112,600 tons of coal equivalent (tce), with oil consumption reaching 3027 tons, 95.4% of which was diesel. Coal and natural gas consumption totaled 35.66 million m^3, while electricity consumption amounted to 956 million kWh. The ecological environment of the study area can be classified into three main types: irrigated areas, desert ecosystems, and the transition zone between irrigated land and desert [26]. Over the past decade, the degradation of natural vegetation in the transition zone has gradually slowed. The harsh climate and frequent human activities threaten the local ecosystem [27,28]. The geographic location in the study area is illustrated in Figure 1.

2.2. Methods

2.2.1. Top-Down Approach for Sectoral Virtual Water Reallocation

The top-down input–output model (IOM) is a macroeconomic analytical tool used to quantitatively study the interdependencies between various sectors within a regional socioeconomic system [29]. It provides a detailed description of the indirect or hidden economic and technical relationships among sectors. Because the structure of a regional socioeconomic system is a major factor influencing resource consumption, many researchers have extended the IOM to resource-based models. In water resource management, these models typically use virtual water flows and transfers between industries to analyze the balance of water supply and demand across sectors. Through the circulation of virtual water, one can trace the economic linkages between industries [30,31]. The extended water input–output model (WIOM) accurately captures virtual water flow across different

industrial sectors within a region, supporting future resource management strategies and trade policies aimed at improving resource efficiency from the perspective of demand-side strategies [32]. In this study, we employed the bi-proportional scaling technique (RAS method) to update and reconstruct the input–output tables (IOT) released by the Xinjiang government [33]. This approach allowed us to compile water resource IOT for the region for the years 2005, 2010, and 2015. The RAS method effectively addresses data gaps in non-census years, requiring minimal data and simplifying the table construction process. We recognize that the reliability of the original data is critical to the success of this method. Therefore, the base data we utilized come from extensive, long-term research conducted in collaboration with various county governments within the study area. These original data sources stem from projects in which we have been actively involved, including field surveys and data collection efforts in partnership with local authorities. This collaborative approach not only enhances the credibility of the data but also ensures its relevance and accuracy in reflecting local economic and environmental conditions. By leveraging these established relationships and prior research, we aim to minimize discrepancies and maximize the reliability of the input–output tables constructed through the RAS method [34]. Following the classification standard of sectors in the IOT [35], we consolidated the 42 sectors in the IOT into 28 sectors to match the available water data (see Appendix A—Table A1). Based on this, the IOM for physical and virtual water transfer and allocation among the economic sectors in the study area is expressed as follows:

$$k + h + y = (I - A)^{-1} \cdot (f_1 + f_2 + e) \quad (1)$$

where k and h represent the intermediate use vectors of locally produced and imported goods in economic production, respectively; $(I - A)^{-1}$ represents the n × n Leontief inverse matrix; and y denotes the final demand vector, which includes government and local household consumption vectors (f_1), capital formation vector (f_2), and export vector (e). Utilizing the formula outlined above, the virtual water transfer matrix for the production and consumption processes across the economic sectors examined in this study is presented in Equation (A1)–(A6) in the Appendix B.

To better illustrate the application of the constructed WIOM, we take cotton production as an example to visualize the transfer and reallocation of both physical and virtual water in the production and consumption processes (Figure 2). From the production side, after cotton is planted and harvested locally, part of it is directly purchased and consumed by the local government and residents as the final users [36]. Another portion is used as raw material in local industries, such as the textile and oil processing sectors, to produce cotton products and cottonseed oil. Additionally, some cotton is exported as raw material to other regions, serving as an intermediate input for external textile processing industries [37]. From the consumption side, the final product consumed is cotton. During its production, inputs such as cotton seeds are required, as well as resources from other sectors like manufacturing, electricity, and wholesale and retail, which provide fertilizers, pesticides, plastic films, agricultural machinery, diesel, and electricity. The virtual water embedded in cotton thus consists of both the local physical water consumed during its production and the virtual water contained in these inputs. This water consumption includes both direct physical water use and indirect virtual water use. The virtual water embodied in fertilizers, pesticides, plastic films, agricultural machinery, diesel, and electricity originates from the physical water consumed by the relevant manufacturing, power, and other sectors. Therefore, this water use during cotton production is an indirect form of water resource consumption [38].

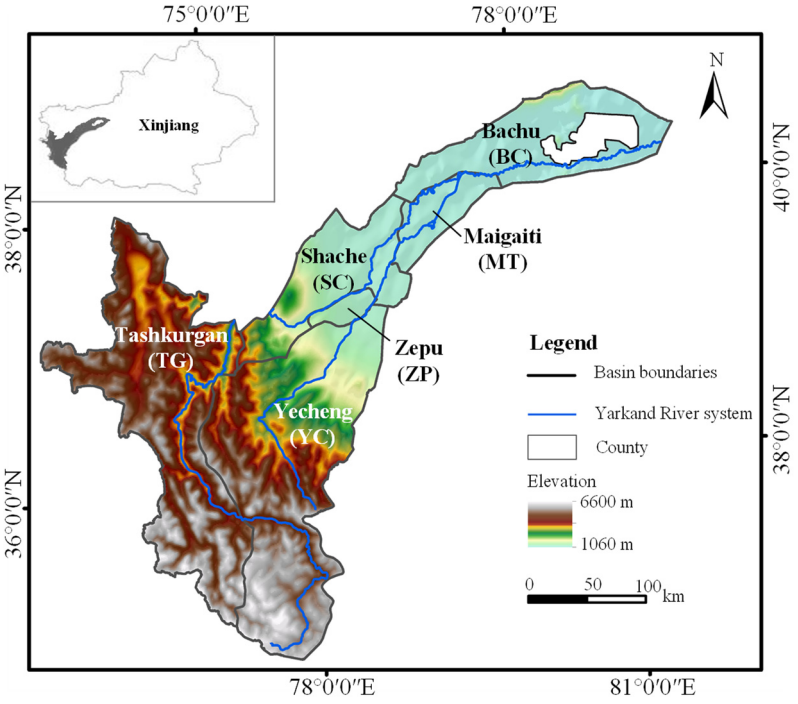

Figure 1. Geographical map of the study area.

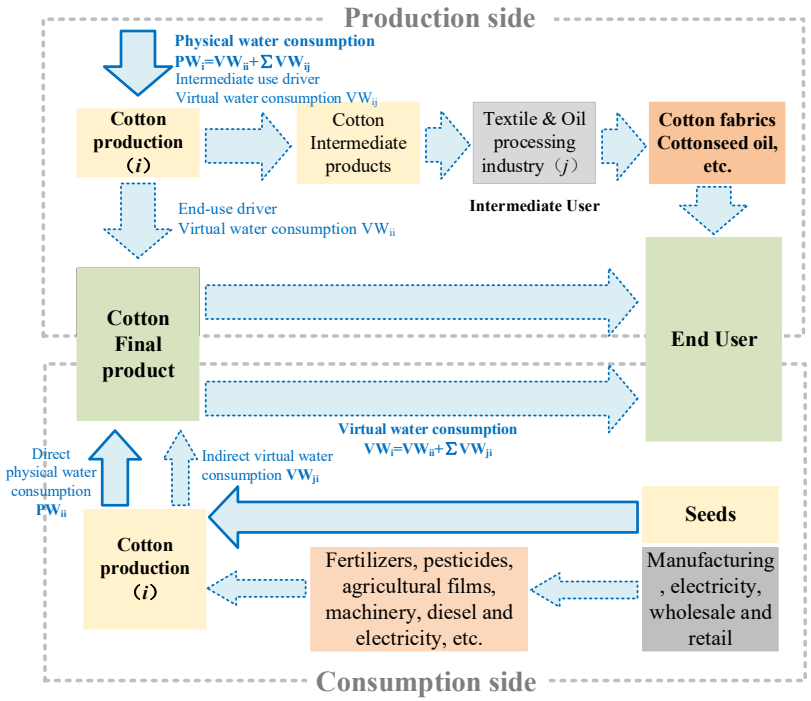

Figure 2. The transfer process of physical water and virtual water during cotton production.

In this study, we further characterize each sector's impact and driving force using the influence correlation coefficient (α_j) and the driving force correlation coefficient (β_i). These coefficients represent the extent to which each sector responds to an increase in the final demand for an initial input of a unit of product and the strength of each sector's contribution to the overall regional economy [39]. The products considered in this analysis

include locally produced goods and those imported from external regions [40]. The specific method is outlined as follows:

$$\alpha_j = \frac{\sum_{i=1}^{n} l_{ij}}{\frac{1}{n}\sum_{j=1}^{n}\sum_{i=1}^{n} l_{ij}} \tag{2}$$

$$\beta_i = \frac{\sum_{j=1}^{n} g_{ij}}{\frac{1}{n}\sum_{i=1}^{n}\sum_{j=1}^{n} g_{ij}} \tag{3}$$

where l_{ij} and g_{ij} are the coefficients from the Leontief inverse matrix and the Ghosh inverse matrix, respectively. The Ghosh inverse matrix, also known as the distribution coefficient matrix $(I - H)^{-1}$, reflects the changes in output across interrelated sectors and the overall socio-economic system through industrial linkage mechanisms. Here, n represents the total number of sectors.

2.2.2. Bottom-Up Approach for Sectoral Water Footprint Accounting

The consumptive water footprint ($wf_{pro(i)}$) for the primary crop systems (i.e., agriculture) in the study area is divided into the blue water footprint and green water footprint for crop production. The classification method is as follows:

$$wf_{pro(i)} = \frac{wf_{blue(i)} + wf_{green(i)}}{x_i} \quad i = 1, 2, \ldots, 10 \tag{4}$$

where $wf_{blue(i)}$ and $wf_{green(i)}$ represent the blue and green water footprint vectors of the i-th subsector, respectively. x_i refers to the total output vector of the i-th subsector, which includes 10 major crops produced in the basin: cotton, wheat, maize, rice, legumes, oil crops, fruits, vegetables, tubers, and alfalfa.

To calculate the effective precipitation during the crop growing season, we employed the CROPWAT model, recommended by the U.S. Department of Agriculture's Soil Conservation Service. Additionally, crop evapotranspiration during the growing season under varying regional and climatic conditions was calculated using the Penman–Monteith method, recommended by the United Nations Food and Agriculture Organization (FAO). The method for calculating the blue water footprint (wf_{blue}) in crop production is as follows:

$$wf_{blue} = CWU_{blue}/Y \tag{5}$$

$$CWU_{blue} = 10 \times \sum_{d=1}^{\lg p} ET_{blue} \tag{6}$$

$$ET_{blue} = \max(0, ET_c - P_{eff}) \tag{7}$$

where CWU_{blue} refers to the blue water used in crop production (m^3/ha), Y represents the yield per unit area (t/ha), ET_{blue} represents the blue water requirement (mm), and the factor 10 is a unit conversion factor for transforming water depth into water volume over a given land area (dimensionless). The symbol $\sum$ represents the cumulative blue water from the planting to harvest period, lg$p$ represents the length of the growing period (days), ET_c represents the crop evapotranspiration during the growing season (mm/ha), and P_{eff} represents the effective precipitation during the growing season (mm/ha).

This study does not account for the direct consumption of local green water by secondary and tertiary industries, nor does it include the direct green water consumption by forestry, animal husbandry, and fisheries within the agricultural sector. It is assumed that only the crop production process directly consumes green water, and the changes in green water consumption caused by blue water consumption are negligible and thus ig-

nored [24]. The method for calculating the green water footprint (wf_{green}) in crop production is as follows:

$$wf_{green} = CWU_{green}/Y \tag{8}$$

$$CWU_{green} = 10 \times \sum_{d=1}^{\text{lgp}} ET_{green} \tag{9}$$

$$ET_{green} = \min(ET_c, P_{eff}) \tag{10}$$

where CWU_{green} refers to the green water used in crop production (m^3/ha), ET_{green} represents the green water requirement (mm), and the other parameters share the same meanings as those used in the blue water footprint calculation.

According to the "shortboard principle" of the grey water footprint proposed by Cao et al. (2014), the grey water footprint is categorized as non-consumptive water use [41]. The amount of water required to assimilate these non-point-source pollutants is non-additive, meaning that the same unit of water can dilute both pollutant *A* and pollutant *B*. Therefore, the grey water footprint of crops (wf_{grey}) is determined by the pollutant requiring the largest amount of water for dilution. The calculation method is as follows:

$$GWF_{np}^{j} = \frac{\alpha_j Q_{all}^{j}}{(C_{\max}^{j} - C_{nat}^{j})} \tag{11}$$

$$wf_{grey} = \max\left[GWF_{np}^{1}, GWF_{np}^{2}, GWF_{np}^{j}\right] \tag{12}$$

where α_j represents the runoff rate (%) of the *j*-th non-point source pollutant, Q_{all}^{j} represents the total application amount of the *j*-th pollutant (kg), $C_{\max}^{j}$ represents the maximum permissible concentration of the *j*-th pollutant (kg/m^3), and C_{nat}^{j} represents the background concentration of the *j*-th pollutant in the environment (kg/m^3).

2.2.3. Carbon Footprint Model Based on Life Cycle Assessment

Given that agriculture is the dominant industry in the study area, this research uses the carbon footprint of local crop production to measure greenhouse gas emissions capacity. The carbon footprint accounting model for crop production follows the IPCC Guidelines for National Greenhouse Gas Inventories (https://www.ipcc.ch/report/, accessed on 25 September 2024). The carbon footprint (*CF*) resulting from agricultural inputs during the crop production process (from planting to harvest) for 10 crops, including cotton, wheat, maize, rice, legumes, oil crops, fruits, vegetables, tubers, and alfalfa, is calculated as follows:

$$CF = \sum_{j=1}^{n} ACI_j \times CEF_j \tag{13}$$

where *CF* is the carbon footprint resulting from agricultural inputs and activities during crop production, measured in kg CO_2-eq/ha. ACI_j represents the quantity of the *j*-th agricultural input used, in kg/ha, and CEF_j represents the greenhouse gas emission factor of the *j*-th input, in CO_2-eq. We utilized general emission factors that have been widely adopted in the existing literature for calculating carbon footprints within the study area. Numerous studies have demonstrated the feasibility of using these general emission factors, especially in regions with similar climatic conditions and agricultural production methods [25,42,43]. This approach ensures that the calculated carbon footprint remains relevant and provides a reliable estimate for our analysis. Furthermore, the emission factors employed are consistent with those from regions that share comparable agricultural practices and climate profiles. As a result, we believe that the use of these generalized factors does not significantly deviate from the overall results or impact the prevailing developmental trends observed in our study. The sources for these emission factors and their specific applications during crop production are listed in Table 1.

Table 1. List of greenhouse gases emission factors and sources.

Emission Source		Emission Factor	Source
Seeds	Cotton	0.35	Ecoinvent database
	Wheat	0.58	
	Maize	1.93	
	Rice	1.84	
	Legumes	0.46	
	oil crops	0.83	
	Fruits	0.31	
	Vegetables	0.08	Hu et al. (2016) [44]
	Tubers	0.10	Ecoinvent database
	Alfalfa	0.27	Liu et al. (2018) [45]
Fertilizer	Nitrogen fertilizer	1.53 t CO_2 eq/t	Walling et al. (2020) [46] Ma et al. (2021) [47] Li et al. (2020) [48]
	Phosphatic fertilizer	1.63 t CO_2 eq/t	
	Potash fertilizer	0.65 t CO_2 eq/t	
	Compound fertilizer	1.77 t CO_2 eq/t	
Pesticide	Insecticide	16.61 t CO_2 eq/t	Ecoinvent database
	Fungicide	10.57 t CO_2 eq/t	
	Seed dressing agent	18.04 t CO_2 eq/t	
	Herbicide	10.15 t CO_2 eq/t	
Labors		0.89	Chinese Life Cycle database
Diesel		4.10 t CO_2 eq/t	Xiong et al. (2016) [49]
Electricity		0.97 t CO_2 eq/kwh	Li et al. (2020) [48]
Plastic mulch		22.72 t CO_2 eq/t	Günther et al. (2017) [50]

Note: In this study, agricultural electricity consumption primarily refers to the electricity used for irrigation. The parameter values are based on data from the northwestern regions of China, including Xinjiang, Gansu, Shaanxi, and Ningxia.

The carbon footprint from direct soil N_2O emissions during crop production is calculated as follows:

$$DF_{N_2O} = F_{sn} \times EF_a \times \alpha \times \gamma \quad (14)$$

where DF_{N2O} is the carbon footprint from direct soil N_2O emissions over the entire crop growing season, measured in kgCO_2-eq/ha. F_{sn} refers to the nitrogen fertilizer application rate, in kg/ha/year. EF_a represents the emission factor for N_2O from soil due to nitrogen application, and for this study, based on the China Climate Change Info-Network (https://www.ccchina.org.cn/Detail.aspx?newsId=43405&TId=59, accessed on 25 September 2024, the same below), the factor is set to 0.0056 N_2O-N/kgN. α represents the conversion factor from N to N_2O, and γ represents the global warming potential of N_2O.

The carbon footprint from indirect soil N_2O emissions is calculated as follows:

$$IDF_{N_2O_i} = F_{sn} \times EF_b \times Frac \times \alpha \times \gamma \quad (15)$$

where IDF_{N2Oi} represents the carbon footprint from indirect soil N_2O emissions during the growing season, measured in kgCO_2-eq/ha. EF_b represents the emission factor for N_2O resulting from nitrogen leaching, runoff, and atmospheric deposition. According to the China Climate Change Info-Network, the emission factors are set at 0.01 and 0.0075 N_2O-N/kg (NH_3-N + NO_x-N), respectively. *Frac* represents the proportion of fertilizer nitrogen volatilized as NH_3 and NH_x (0.1 kg/kg) and the proportion of nitrogen lost in soil leaching and runoff (0.3 kg/kg).

Thus, the total carbon footprint from soil N_2O emissions is as follows:

$$CF_{N_2O} = DF_{N_2O} + IDF_{N_2O_i} \quad (16)$$

where CF_{N2O} represents the total carbon footprint from soil N_2O emissions over the entire crop growing season, measured in kgCO_2-eq/ha.

The total greenhouse gas emissions from the entire life cycle of the primary crops in the study area are calculated as follows:

$$CF_{Total} = (CF + CF_{N_2O}) \times A \quad (17)$$

where CF_{Total} represents the total greenhouse gas emissions from the entire life cycle of the major crops, in kg CO_2-eq, and A represents the crop planting area, in hectares (ha).

2.3. Data Description and Processing

The study period spans from 1990 to 2015. Due to data limitations, the analysis of virtual water consumption and allocation focuses on three representative years: 2005, 2010, and 2015. Economic data on sectoral production, import–export trade, and consumption for updating the IOT of the YRB are from the Statistic Bureau of Xinjiang Uygur Autonomous Region and the statistical yearbooks of individual counties in Xinjiang. Data on blue public water consumption for forestry, animal husbandry, and fisheries in the primary industry come from the Xinjiang Water Resources Bulletin released by Xinjiang Uyghur Autonomous Region Government (https://slt.xinjiang.gov.cn/, accessed on 25 September 2024). For the secondary and tertiary industries, blue public water consumption is estimated using data on "water consumption per unit of GDP", "water consumption per unit of added value", "industrial water use quotas", and "major product output", all sourced from the Statistic Bureau of Xinjiang Uygur Autonomous Region. To ensure the reliability and accuracy of these estimates, we conducted cross-validation with data from prior studies and our own field surveys conducted in collaboration with local government agencies. Additionally, consistency checks were performed on data from different sources to eliminate potential conflicts. For major crops extensively cultivated in the region, such as cotton, wheat, and maize, substantial research has been conducted on crop parameters and soil characteristics. We have utilized these established parameters in our model to enhance accuracy [51,52]. Crop growth parameters are additionally derived from the CROP Database of the FAO, which provides comprehensive production statistics for 173 major crops globally, including harvested area, yield, and yield per unit area. For less extensively cultivated crops, such as oil crops and tubers, where research is limited, we opted to use existing parameters in the model, as these crops account for less than 10% of the cultivated area. This ensures that their impact on the overall results is minimal. Industries included in the primary, secondary, and tertiary sectors are detailed in Appendix A—Table A1. Data on effective irrigation areas, crop yields, and other production metrics are obtained from the Statistic Bureau of Xinjiang Uygur Autonomous Region. Meteorological data, including precipitation, sunshine hours, and temperature, are obtained from five meteorological stations within the study area. Data related to agricultural capital inputs—such as fertilizers, pesticides, plastic mulch, and seeds—and agricultural activities, including electricity for irrigation, diesel use, and machinery, are sourced from the Statistic Bureau of Xinjiang Uygur Autonomous Region. Greenhouse gas emission parameters for crop production are taken from existing literature, with detailed sources provided in Table 1.

3. Results and Discussion

3.1. Consumption and Structural Characteristics of Physical and Virtual Water in Different Sectors

Table 2 presents the overall structural characteristics of physical and virtual water consumption across industries in the YRB for 2005, 2010, and 2015. The findings indicate that the primary sector's total volume of physical water consumption consistently accounts for over 98% of the total physical water consumption across all regional sectors. Furthermore, the primary sector continues to lead in virtual water consumption, with most of the virtual water inflow also originating from this sector. Among all sectors, the primary industry in the study area is a net exporter of virtual water, while the secondary and tertiary sectors serve as net importers. In 2005, the net transfer of virtual water from the primary sector was -8.762×10^8 m^3, representing 22.6% of the primary sector's total physical water consumption. This virtual water volume transfers to other sectors, typically

raw materials or intermediate products. Conversely, the net transfer of virtual water from the other sectors was positive, indicating that their virtual water consumption during production exceeded their use of local physical water and incoming virtual water. By 2010, the net transfer of virtual water from the primary sector increased to -18.011×10^8 m^3, although this value slightly decreased to -15.205×10^8 m^3 by 2015. This trend highlights the primary sector's persistent and significantly higher dependence on local real water resources than the secondary and tertiary sectors, resulting in a notably homogeneous water usage structure within the region.

Table 2. Physical water and virtual water consumption by economic sectors (unit: 10^8 m^3).

Sector	Time	Physical Water Consumption	Virtual Water Consumption	Off-Site Virtual Water Consumption	Net Virtual Water Transfer	Virtual Water Outflow
Primary industry	2005	38.708	29.946	0.774	−8.762	28.221
	2010	53.635	35.624	1.073	−18.011	33.091
	2015	51.745	36.540	1.035	−15.205	33.316
Secondary industry	2005	0.085	7.363	0.014	7.278	0.070
	2010	0.498	14.689	0.046	14.192	0.602
	2015	1.025	14.604	0.066	13.580	8.507
Tertiary industry	2005	0.491	1.975	0.172	1.484	0.354
	2010	0.602	4.422	0.211	3.819	0.032
	2015	0.050	1.676	0.017	1.625	0.314

Based on the results mentioned, we further refined our calculations of physical and virtual water consumption, as well as outflow ratios for the 28 subsectors in the YRB, and analyzed the annual variation rates of virtual water consumption (Figure 3). Between 2005 and 2010, D28 was the second-largest consumer of physical water, following D1, accounting for approximately 0.8% of total consumption. By 2015, however, the share of physical water consumption by D28 had declined to 0.1%. In contrast, D23 maintained a physical water consumption share of less than 0.1% during 2005 and 2010 but became the second-largest consumer by 2015, rising to 1.2%. D1 consistently accounted for over 65.1% of virtual water consumption, peaking at 76.2% in 2005. D6 was the second-largest contributor to virtual water consumption in the YRB, with its share fluctuating between 5.6 and 10.3%. Notably, D7 and D8 showed a significant upward trend in their virtual water consumption, while the share from the tertiary sector gradually decreased. Regarding virtual water outflow, D1 represented over 96.5% of the total virtual water outflow from the region's industries. Both the first and third sectors exhibited a decline in their shares of physical and virtual water consumption and virtual water outflow, whereas the second sector showed the opposite trend. These findings indicate that total virtual water consumption in the basin's sectors increased by 25.6% from 2005 to 2015. However, the proportion of virtual water sourced from external regions within D1 did not change significantly; consumption increased by only 25.1% compared with 2005. In contrast, the second sector experienced a substantial increase of 79.5%, suggesting that the development of the second sector increasingly relied on external products and services. Examining the annual variation rates of virtual water consumption from 2005 to 2010, we observed that three subsectors (D6, D23, and D27) experienced negative growth rates of −5.3, −8.3, and −2.6%, respectively. Conversely, the largest growth rate was seen in D19, reaching 216.5%. From 2010 to 2015, eight subsectors demonstrated positive growth in virtual water consumption, with D23 exhibiting the highest growth rate of 104.2%. This further underscores the observation that these sectors directly consumed significantly more local physical water than they relied on virtual water sources.

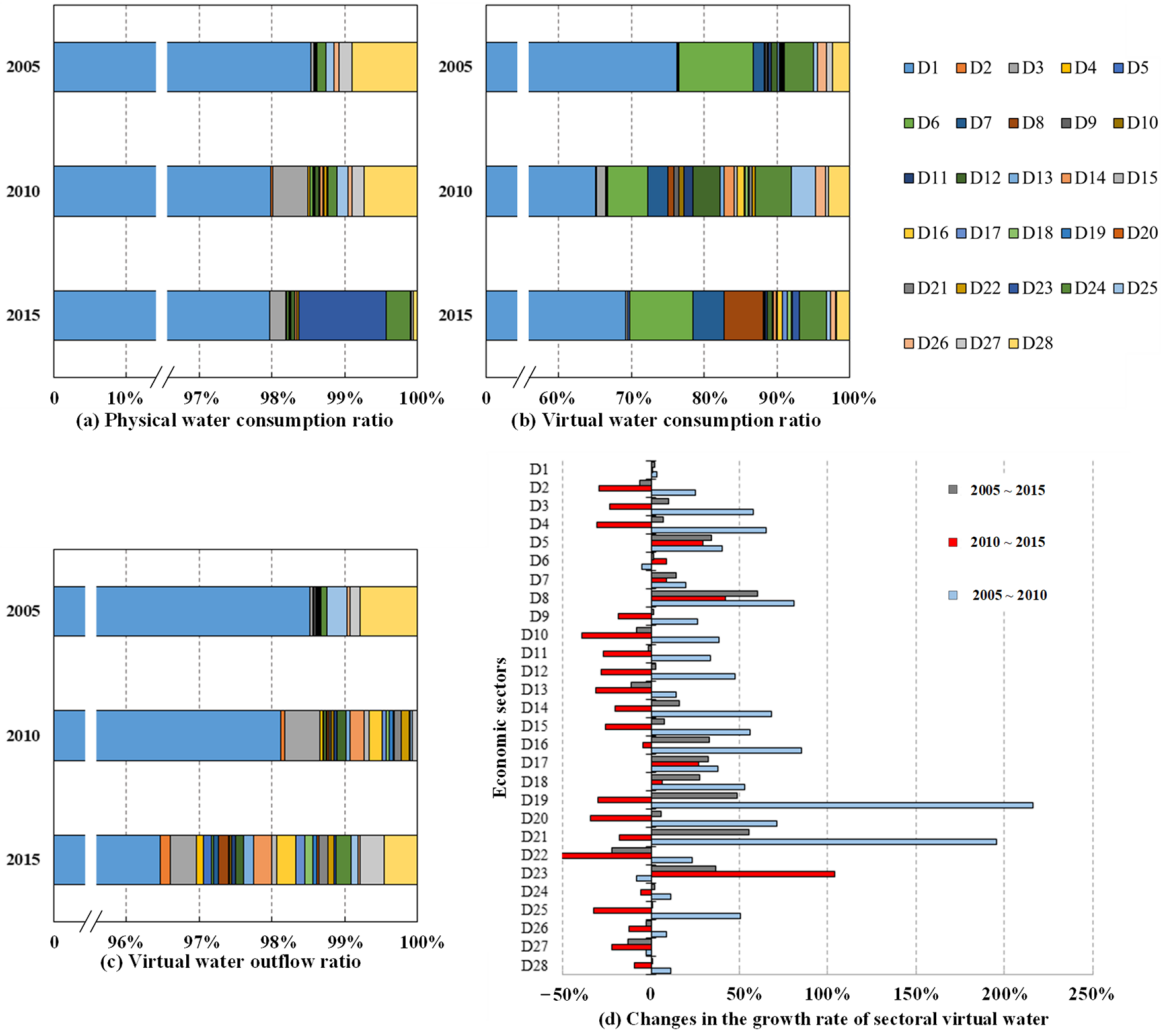

Figure 3. Changes in the structure of physical water and virtual water consumption.

The study area has consistently demonstrated a crop-dominated industrial structure. We conducted a spatial analysis of blue and green water consumption in the 10 subsectors of the planting industry within the study area for the years 2005, 2010, and 2015, as well as the scale of planting in each county and their corresponding water consumption (Figure 4). The results indicate that the total blue water consumption of the planting industry subsectors increased from 2.056 billion m^3 in 2005 to 3.805 billion m^3 in 2015. Among these, cotton (c5) had the largest share of blue water consumption, accounting for an average of 45.3%. Wheat (c2) and maize (c3) followed, with shares of 21.1 and 18.4%, respectively. The remaining subsectors each accounted for less than 6% of total blue water consumption. In terms of green water consumption, c5 again had the highest average share at 46.1%, followed by c2 at 20.8% and c3 at 18.2%. Spatially, SC had the largest planting scale and the highest total blue and green water consumption among the six counties studied. The county's crop planting area represented 34.1 to 38.9% of the total area in the study region, with c5 accounting for 52.4% of the total blue and green water consumption. The planting industries of MG and BC were also dominated by c5, with cotton accounting for 64.3 and 61.7% of total blue and green water consumption, respectively. In YC, the main crops were c2 and c3, with these grains accounting for 27.3 and 25.3% of the local planting industry, respectively. ZP's largest planted crop was legumes (c4), covering 37.2% of the cultivated area, although its blue and green water consumption was lower than that of c5. TG had the smallest planting scale and the lowest total blue and green water consumption among the counties. In summary, the YRB is transitioning from a crop structure dominated by

grains like c2, c3, and c4 to an economic crop structure dominated by c5. This shift reflects an increasing focus on crops with higher economic returns and highlights the growing demand for blue and green water resources in the region [51].

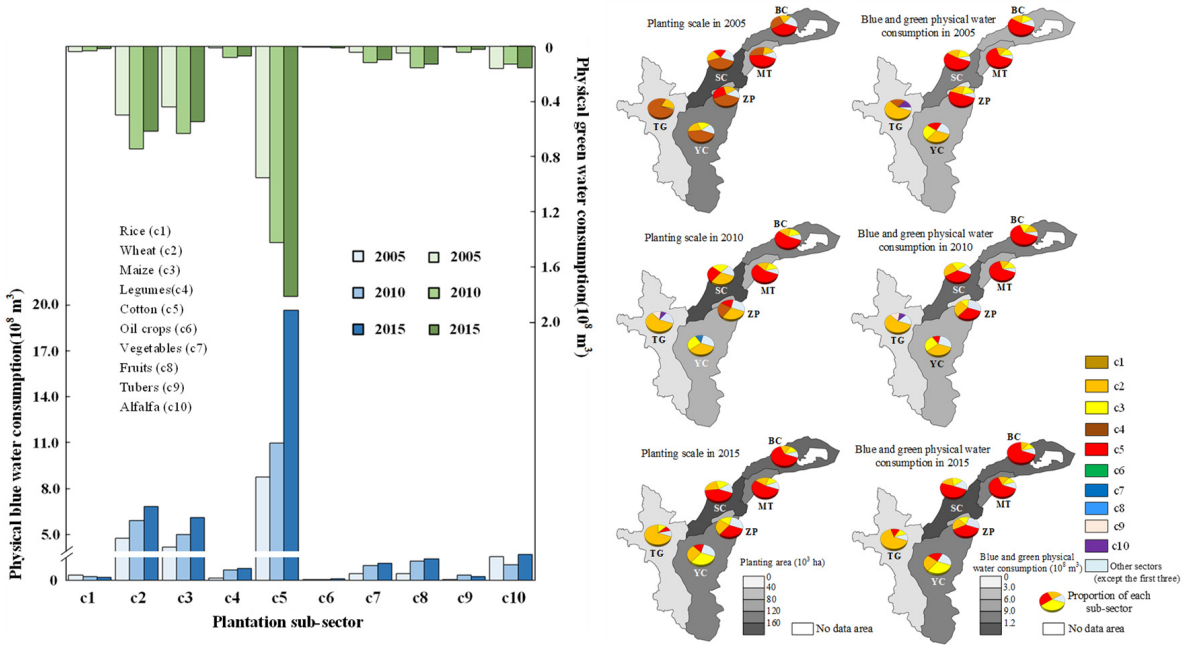

Figure 4. The scale of different planting subsectors and the spatial distribution of blue–green physical water consumption.

3.2. Evolution Path and Driving Forces of Sectoral Virtual Water

Figure 5 illustrates the interactions of blue and green virtual water among various economic sectors in 2015. The width of the virtual water flows represents the volume of water transferred, where a wider flow indicates a larger transfer volume. The inner ring of the figure shows the absolute scale of these transfers, while the outer ring indicates the proportion of the total virtual water transferred between sectors. The volume of transferred virtual water between sectors also reflects the degree of water consumption linkage among them.

Across the three periods, there are common characteristics in the flow and transfer of blue and green virtual water between sectors. However, changes in the local policy direction for the relevant industries have altered the state of virtual water transfers and the degree of association between certain sectors. One consistent feature is that D1 has the largest internal allocation of virtual blue water, with around 1.90×10^8 m^3, accounting for 54.7% of the total direct blue water consumption. The remaining virtual blue water was transferred to other sectors. Compared with D1, the net transfer of virtual blue water from the other 27 sectors was significantly smaller (the second highest was less than 46% of D1's transfer). These sectors allocated less than 40% of their total water consumption to the internal use of virtual blue water, with the tertiary sector, represented by D28, only allocating 30.4% of its total blue water consumption to internal distribution. This pattern highlights the observation that blue water is the primary source of virtual water for other sectors, while D1 exhibits a higher output and transfer of virtual blue water. The top three recipients of D1's virtual blue water transfer are D6, D8 and D7, with transfer volumes of 4.08×10^8, 2.46×10^8, and 1.96×10^8 m^3, respectively. This indicates that the share of virtual blue water transferred from D1 to sectors such as food, textiles, and apparel manufacturing industries has been increasing, implying that the expansion of D1 directly contributes to higher water consumption intensity in these sectors. Apart from D1, the transfer of virtual blue water is gradually shifting from "energy-intensive" sectors to "labor-intensive" sectors. The internal allocation of virtual green water for D1 was approximately 2.30×10^8 m^3,

accounting for 59.9% of total direct green water consumption. Similarly, the amount of virtual green water transferred from D1 to food, textiles, and apparel manufacturing and related service sectors was much higher than the transfers to other sectors. The combined transfer volume of virtual green water from D1 to these sectors exceeds 50% of its total virtual green water transfer.

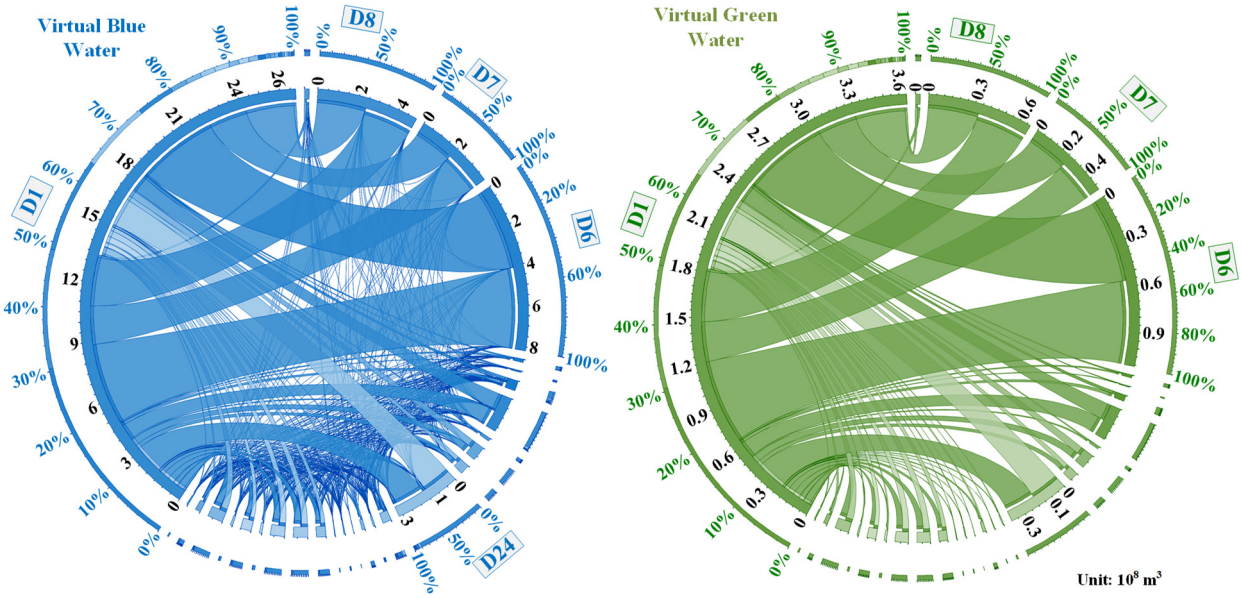

Figure 5. Flow and transfer of blue–green virtual water among sectors in 2015.

As discussed in Section 3.1, both the production and consumption perspectives show that the intermediate use of blue and green water in cotton production was the highest. This result also reflects the substantial indirect contribution of cotton cultivation to the consumption of blue and green virtual water by other economic sectors in the study area [53]. D1 receives relatively little virtual water from external products compared with its local blue and green water consumption, while other sectors have a high demand for the virtual water embedded in external D1 products (or services). Therefore, importing virtual water through the trade of external products from the secondary and tertiary sectors may serve as a strategy by which to mitigate D1's excessive consumption of local virtual water. Additionally, D1 is the primary supplier of blue and green virtual water in production, while sectors such as food, textiles, and apparel manufacturing exhibit the highest levels of indirect consumption of the blue and green virtual water embedded in D1's products (or services).

Figure 6 illustrates the influence correlation coefficient (α_j) and the driving force correlation coefficient (β_i) for six major industry categories in the YRB. The top three industries with the most decisive influence and driving effects are ranked in descending order, represented by red, blue, and green bars in the corresponding stacked bar chart. The grey segments represent the combined influence of the other three industries. The results show that, compared with other industries, the construction industry (v) and agriculture (i) exhibited cumulative influence values ($\alpha_j > 1$) that exceed the system average. In both cases, their cumulative α_j values were higher than their cumulative β_i values, indicating a strong dependence on the products or services of other industries, particularly the processing and manufacturing industry (iii) and the service industry (vi). Although agriculture (i) accounts for the majority of virtual water consumption in the YRB, it only exerts a moderate influence on the local processing and manufacturing industry (iii), ranking behind the service industry (vi) in terms of its α_j. Furthermore, the construction industry (v), processing and manufacturing industry (iii), and agriculture (i) showed cumulative driving force values ($\beta_i > 1$) above the system average. However, unlike construction and agriculture, the

cumulative β_i value of the processing and manufacturing industry exceeds its cumulative α_j value. This suggests that an increase in the final use of the manufacturing sector's outputs leads to higher water consumption in the industries that rely on its products, indicating that the manufacturing sector has lower water-saving potential than others in the region. Aside from agriculture (i), local energy production and water supply are primarily concentrated in the mining and extraction industry (ii) and in the energy and power industry (iv). These industries have lower α_j and β_i values than other industries, as they were less directly reliant on agricultural products. This indicates that these two industries operate relatively independently and have higher water storage capacity than others.

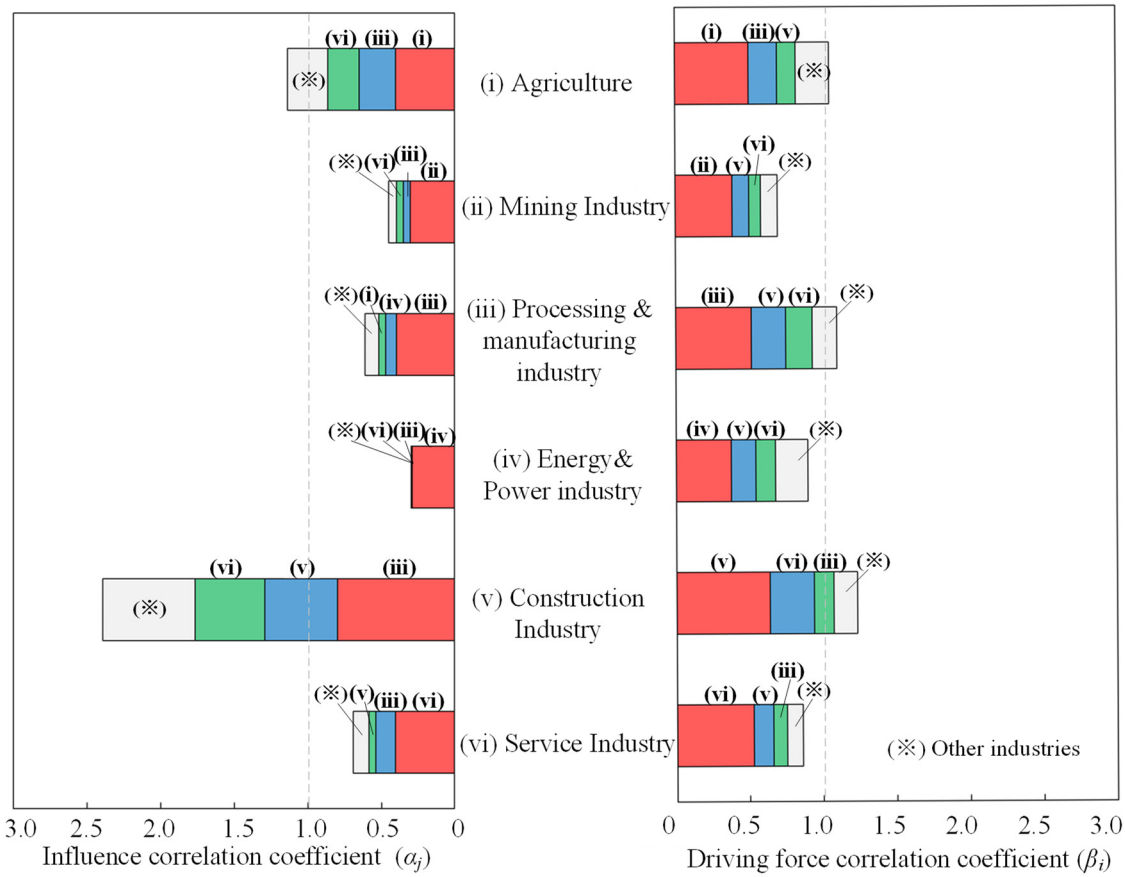

Figure 6. The influence and driving force correlation coefficient of the dominant industry.

3.3. Composition and Spatiotemporal Analysis of Water–Carbon Footprints in the Planting Industry

We adopted a "bottom-up" analytical approach to examine the evolution and characteristics of the water footprint of planting activities in the YRB from 1990 to 2015 (Figure 7). The results indicate that the water footprint per unit of production (*WFP*) fluctuated between 0.68 and 2.10 m^3/kg, with a gradual declining trend over time, though the annual variations were relatively small. Between 2010 and 2015, the average WFP_{blue} and WFP_{grey} were 41.5 and 33.4%, respectively, of their levels between 1990 and 2000. This reduction is closely related to the widespread adoption of efficient water-saving agricultural technologies promoted by local governments after 2008 [54]. These findings demonstrate that the implementation of such technologies can effectively reduce *WFP* by minimizing blue water usage in inefficient irrigation systems and by reducing water evaporation. The spatial variation of *WFP* across counties over the 25-year period reveals notable differences. The average *WFP* ranked as follows: TG (2.17 m^3/kg) > MT (1.80 m^3/kg) > BC (1.75 m^3/kg) > SC (1.45 m^3/kg) > ZP (1.33 m^3/kg) > YC (1.15 m^3/kg). Among these, YC and ZP had annual *WFP* values lower than the YRB's average (1.45 m^3/kg), indicating that they used

relatively less water per unit of crop production. In contrast, TG's average *WFP* exceeded the regional average by 1.50 times, which can be attributed to differences in local climate, cropping patterns, irrigation practices, and agricultural development levels [55].

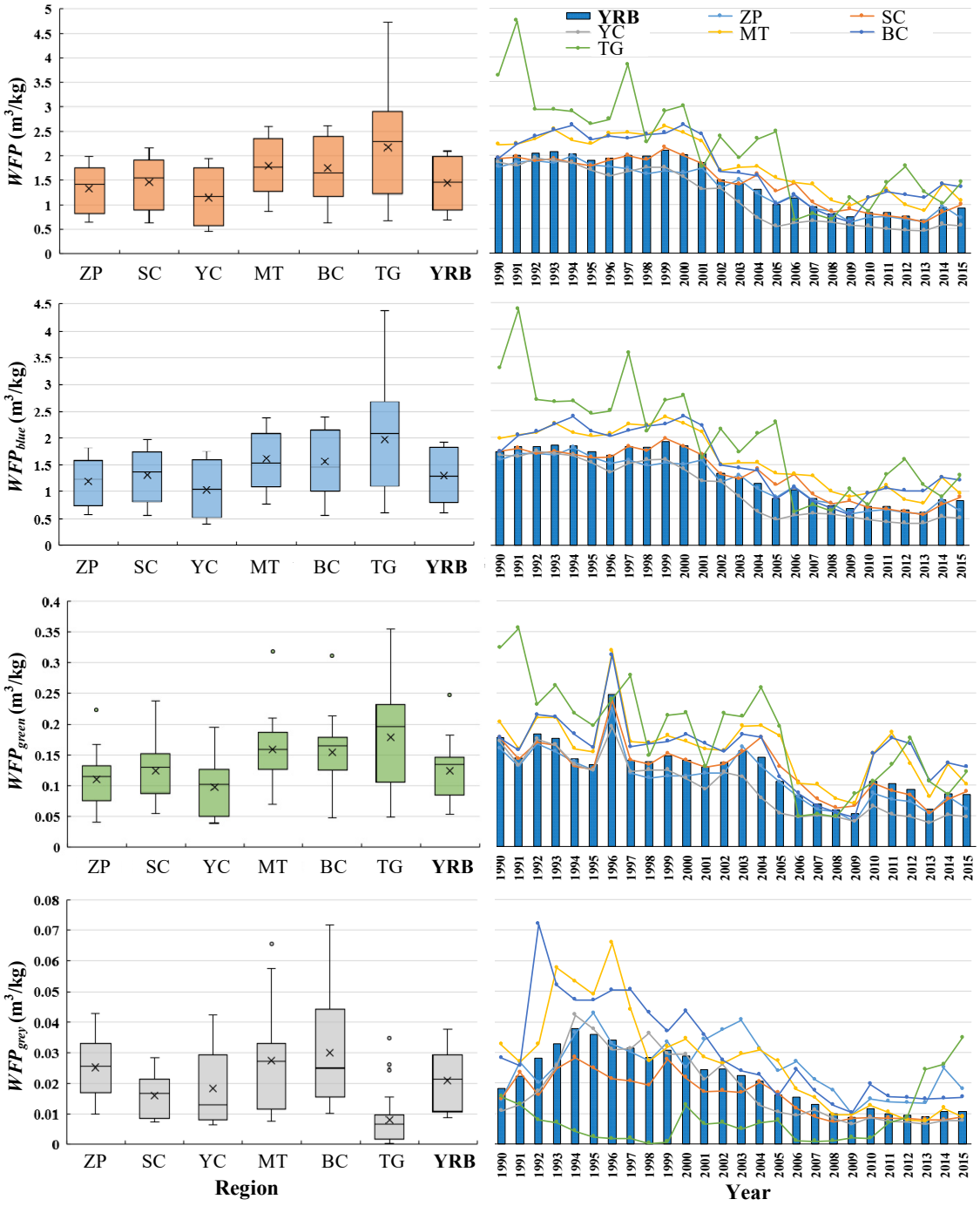

Figure 7. Temporal and spatial changes of crop production water footprint from 1990 to 2015.

In comparison with WFP_{green} and WFP_{grey}, WFP_{blue} exhibited greater interannual variability across counties. During the early 1990s, irrigation methods primarily relied on flood, border, and furrow irrigation, resulting in an upward trend in WFP_{blue} during this period [56]. However, as crop cultivation practices, water-saving irrigation technologies (particularly drip irrigation), and irrigation systems improved, agricultural water-use efficiency significantly increased across counties. After 2000, major agricultural counties such as BC, SC, and MT saw marked declines in WFP_{blue}. These advancements in irrigation

techniques have contributed to the sustainability of water usage in the crop production chain, ensuring that, despite increasing crop yields, the amount of water required per unit of crop output remained relatively low. We compared the *WFP* for the YRB with relevant data from previously published data related to similar investigations (Table 3). Our analysis indicates that the *WFP* of the YRB is at a moderate level compared with the national average.

Table 3. Comparison of the *WFP* in the study area with other regions (unit: m^3/kg).

Time Span	Comparison Area	*WFP*	Source
1990–2015	Southern Xinjiang	2.56	Zhang et al. (2018) [57]
2000–2010	Hetao irrigation area of Inner Mongolia	1.56	Cao et al. (2014) [41]
1990–2012	Arid inland river areas of northwestern China	1.53	Wu et al. (2017) [58]
1990–2015	Hainan Province	2.41	
1990–2015	Shandong Province	0.77	Cao et al. (2018) [59]
1990–2015	China	1.24	

Based on the crop yield statistics from the six counties within the study area, combined with the previously calculated *WFP* results, a further analysis of the total crop water footprint (wf_{total}) was conducted. The interannual trends in wf_{total} for each county from 1990 to 2015 are shown in Figure 8. The results indicate an overall upward trend in wf_{total} across all counties over time. Among the components, the interannual fluctuations and growth rate of wf_{blue} were more pronounced compared with wf_{green} and wf_{grey}, with increases in wf_{blue} ranging from 0.15×10^8 to 7.01×10^8 m^3. In contrast, wf_{green} and wf_{grey} exhibited slower, more gradual increases, with increments of 0.02×10^8 to 0.92×10^8 m^3 for wf_{green} and 0.01×10^8 to 0.10×10^8 m^3 for wf_{grey}. These findings suggest that wf_{blue} plays a dominant role in determining wf_{total} in each county. As a result, variations in wf_{blue} directly influence the water resources consumed by crop production.

Over the past 25 years, several distinct peaks in wf_{total} have been observed across the counties. The causes of these peaks can be attributed to two main factors: first, the dual demands of national food security and regional economic growth [60] and, second, the comprehensive efforts by the central government to promote and deepen the development of advantageous industries, poverty alleviation, and interregional support policies in southern Xinjiang [61]. The rapid expansion of crop cultivation in these counties has increased water stress, particularly in the context of agricultural production and related industrial growth.

Based on the analytical methods in Section 2.2.3, we calculated the total greenhouse gas emissions (GHG_{total}) generated during crop production in the YRB and examined the composition of its carbon footprint (*CF*) (Figure 9). From 1990 to 2015, GHG_{total} increased from 1.88×10^8 $kgCO_2$-eq to 24.81×10^8 $kgCO_2$-eq, representing a 12.2-fold increase with an average annual growth rate exceeding 11.3%. Both direct and indirect emissions from various agricultural inputs and practices showed varying degrees of increase. Notably, the GHG emissions from electricity consumption in agricultural production ($GHG_{electricity}$) increased the most, by 11.27×10^8 $kgCO_2$-eq, followed by emissions from plastic mulch usage (GHG_{mulch}), which increased by 4.26×10^8 $kgCO_2$-eq. Given that large-scale drip irrigation under plastic mulch was introduced in the YRB after 2000 [62], the emissions from plastic mulch were calculated based on changes from 2000 to 2015. The sharp rise in electricity use and the extensive use of plastic mulch in agricultural production after 2000 were key drivers of the increasing trend in GHG_{total}. In contrast, the emissions from pesticide use ($GHG_{pesticide}$) increased the least, by 0.13×10^8 $kgCO_2$-eq. The *CF* of crop production showed a significant upward trend between 1990 and 2015 ($p < 0.01$), with substantial interannual fluctuations. Over the 25-year period, CF_{total} experienced three distinct phases: 1990–1999, 2000–2003, and 2004–2015. During 1990–1999,

fluctuations were relatively moderate, with CF_{total} ranging from 716.49 to 1452.40 $kgCO_2$-eq/hm^2, peaking in 1997 (1452.40 $kgCO_2$-eq/hm^2). The fluctuations became more pronounced between 2000 and 2003, with a range of 669.91 $kgCO_2$-eq/hm^2 and a peak in 2001 (1905.50 $kgCO_2$-eq/hm^2). From 2004 to 2015, although CF_{total} exhibited smaller fluctuations, its upward trend was more prominent than in the previous two periods, with a net increase of 2933.25 $kgCO_2$-eq/hm^2 over the decade, reaching a maximum of 4246.83 $kgCO_2$-eq/hm^2 in 2015.

Regarding the composition of the *CF*, the proportion of emissions from seed inputs, pesticide use, and diesel consumption remained relatively stable, fluctuating between 2.5 and 7.6%. The largest contributor was soil N_2O emissions, with an average share of 28.6% over the years. This includes direct N_2O emissions from soil, indirect emissions from nitrogen leaching and runoff, and atmospheric nitrogen deposition. The second-largest contributor was fertilizer input, with an average share of 24.2%. However, both soil N_2O and fertilizer inputs displayed a significant downward trend over the 25-year period, with their shares decreasing from 37.6 and 31.5% in 1990 to 13.0 and 10.5% in 2015, respectively. After 2000, plastic mulch accounted for approximately 25.7% of the *CF* of crop production in the region.

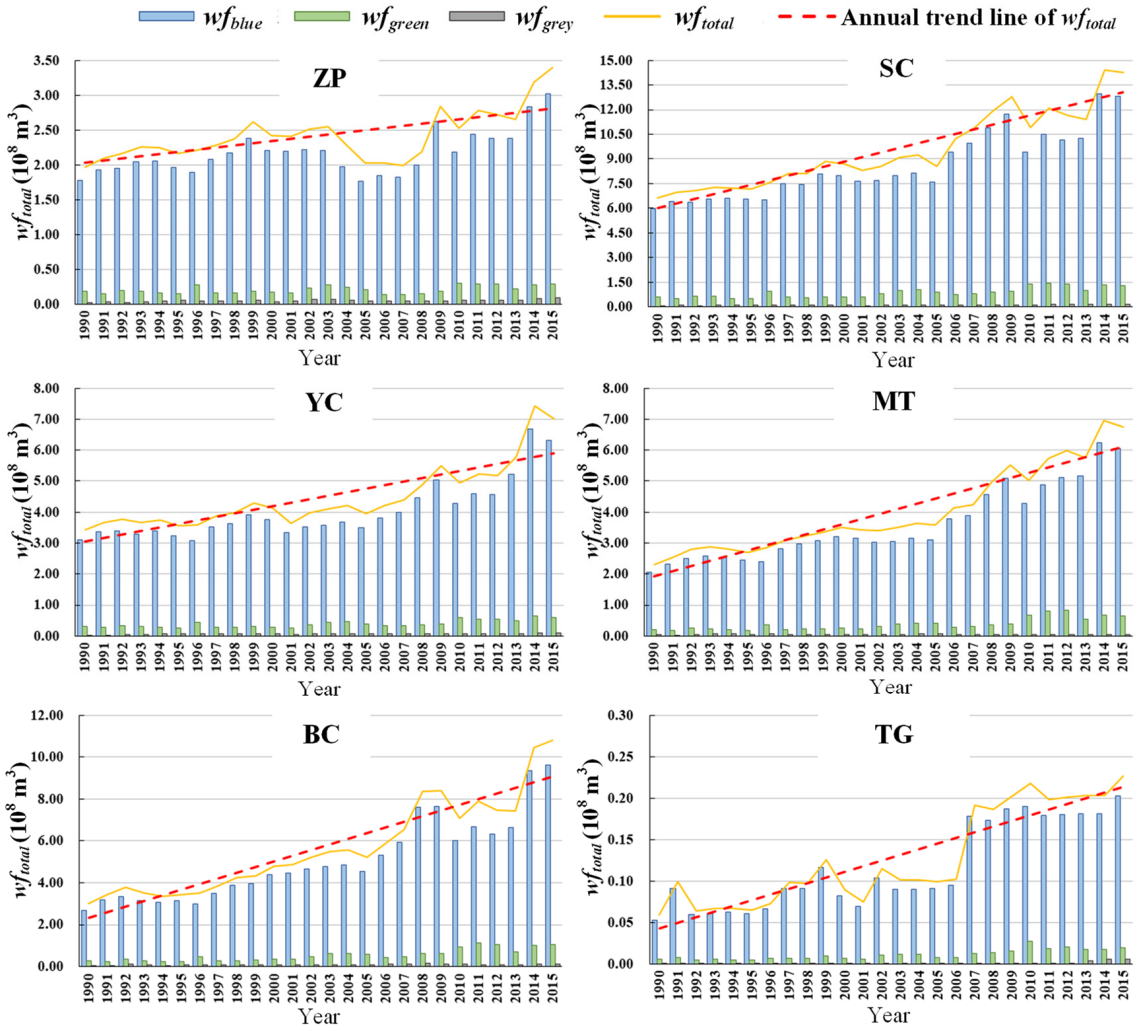

Figure 8. The interannual variation trend of crop water footprint by county-level administrative regions from 1990 to 2015.

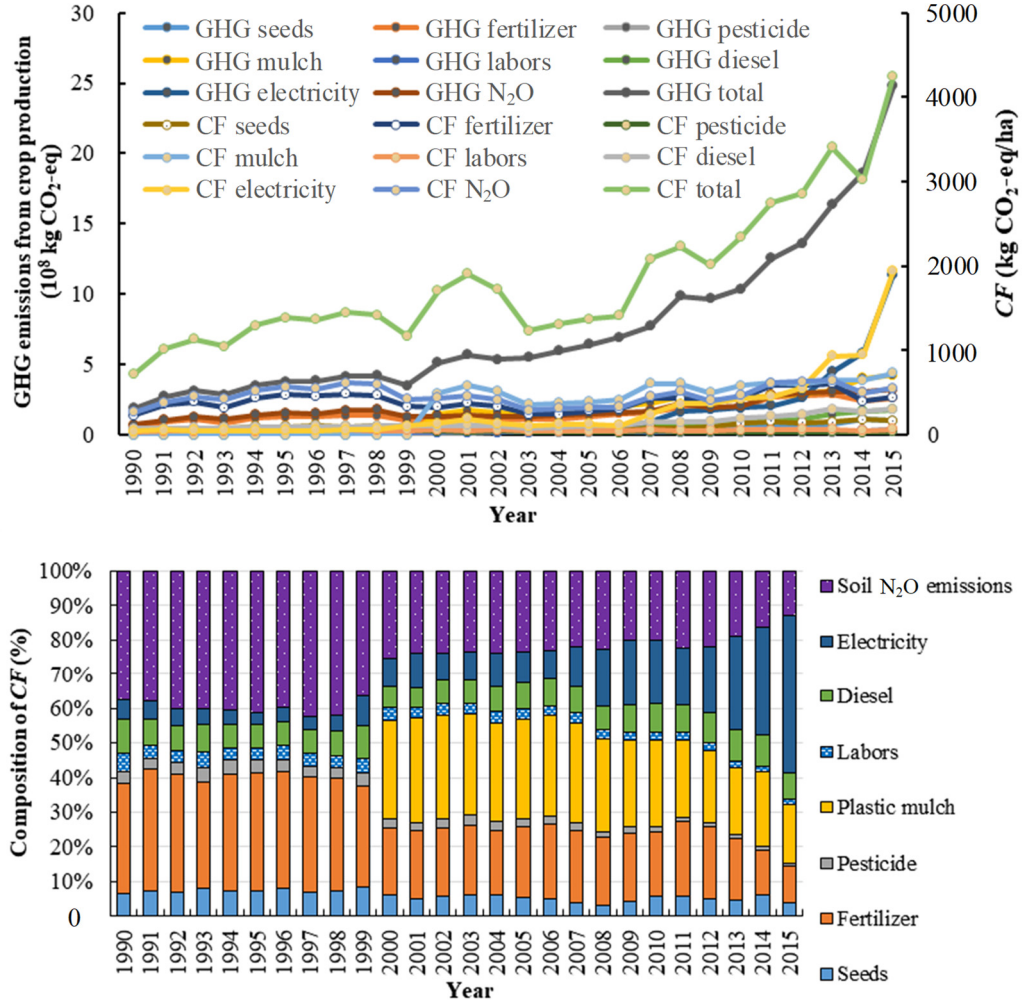

Figure 9. Changes in GHG emissions and carbon footprint (*CF*) composition from crop production between 1990 and 2015.

Meanwhile, the contribution of electricity consumption to *CF* increased dramatically, from 5.5% in 1990 to 45.8% in 2015, and this trend is expected to continue. Therefore, soil N_2O emissions have been a major driver of the increased greenhouse gas intensity in the YRB. Notably, the growing impact of electricity usage on *CF* highlights the need to improve the efficiency of inputs such as electricity and plastic mulch to mitigate GHG emissions. Given the high capital investment, intensive agricultural practices, and substantial output in the region, optimizing the use of these inputs is critical for reducing both greenhouse gas intensity and total emissions [25].

Between 1990 and 2015, significant differences in the *CF* of crop production were observed across counties in the YRB, with an average *CF* of 1923.45 kg CO_2-eq/hm^2 (Figure 10). The highest value was recorded in BC, at 2767.27 kg CO_2-eq/hm^2, followed by MT (2389.42 kg CO_2-eq/hm^2) and ZP (2347.30 kg CO_2-eq/hm^2). Spatially, counties located in the upstream regions, such as YC and TG, exhibited significantly lower *CF* per unit of cultivated area and per unit yield compared with downstream counties like BC, MT, and ZP. In counties with relatively high *CF* values, such as BC and MT, electricity use for agricultural production contributed the most to GHG emissions, accounting for 33.5 and 25.2%, respectively. Plastic mulch usage ranked second, with contributions of 19.0 and 21.8%, respectively. In other counties, such as ZP, TG, and SC, electricity for agricultural activities also contributed over 10% to GHG emissions. In YC, where agricultural production was on a smaller scale, direct emissions of soil N_2O and nitrogen fertilizer application were the primary contributors to GHG emissions, contributing

20.4 and 13.4%, respectively. A comparison of the *CF* composition across counties reveals notable differences in the contribution of various agricultural inputs and activities. Across the entire study area, fertilizer contributions to *CF* followed the following order: nitrogen > phosphorus > compound fertilizer > potassium. This pattern was found to be consistent in counties such as ZP, YC, and MT, while in other counties, slight deviations were observed. Notably, in BC and TG, phosphorus fertilizer made the largest contribution to the fertilizer-related *CF*. The *CF* contribution of soil N_2O emissions in agricultural lands across the study area followed the following order: direct soil N_2O emissions > indirect emissions from nitrogen leaching and runoff > indirect emissions from atmospheric nitrogen deposition. This reflects that the significant use of plastic mulch and nitrogen fertilizer was a major factor in the higher proportion of direct soil N_2O emissions.

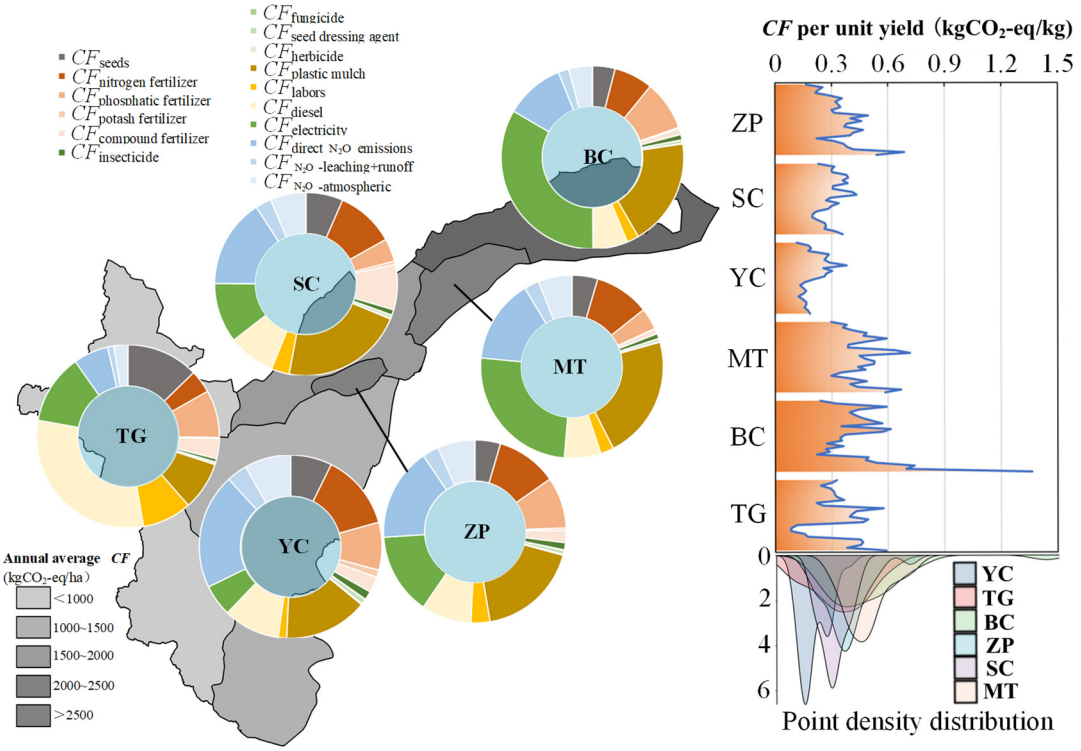

Figure 10. Composition and trends of the carbon footprint (*CF*) from crop production in each county.

The growing pressure of GHG emissions from crop production is closely linked to the scale of agricultural activities and the increasing reliance on agricultural inputs [63]. As the dependence on fertilizers and other inputs in crop production, particularly for cotton, continues to rise, an increase in total GHG emissions is inevitable. Between 2013 and 2015, the *CF* per unit yield in BC surpassed the national average (0.890 kg CO_2-eq/kg), and the values in MT and ZP were approaching the national average during the same period. These counties are the primary sources of GHG emission pressure in the YRB. It is noteworthy that TG, located upstream with a relatively small contribution to GHG emissions from crop production, experienced a sharp 6.95-fold increase in *CF* per unit yield between 2006 and 2015. This suggests that the intensive agricultural GHG emissions in the downstream regions have begun to affect the upstream environment.

3.4. Synergistic Mechanism Based on the Interaction Between Sectoral Water Consumption and Environmental Emissions

3.4.1. Framework for the Industry Water–Carbon Linkage and Policy Impact

The production activities in the study area exhibit an overall upward trend in the complete consumption of water resources and GHG emissions. Changes in the water–carbon footprint are crucial long-term factors influencing local resource utilization and

management. To address this, a comprehensive evaluation framework for the reverse linkage characteristics and driving mechanisms of agricultural water–carbon footprints must be constructed. This framework will consider human and resource inputs, production scale, and relevant policy regulations (Figure 11).

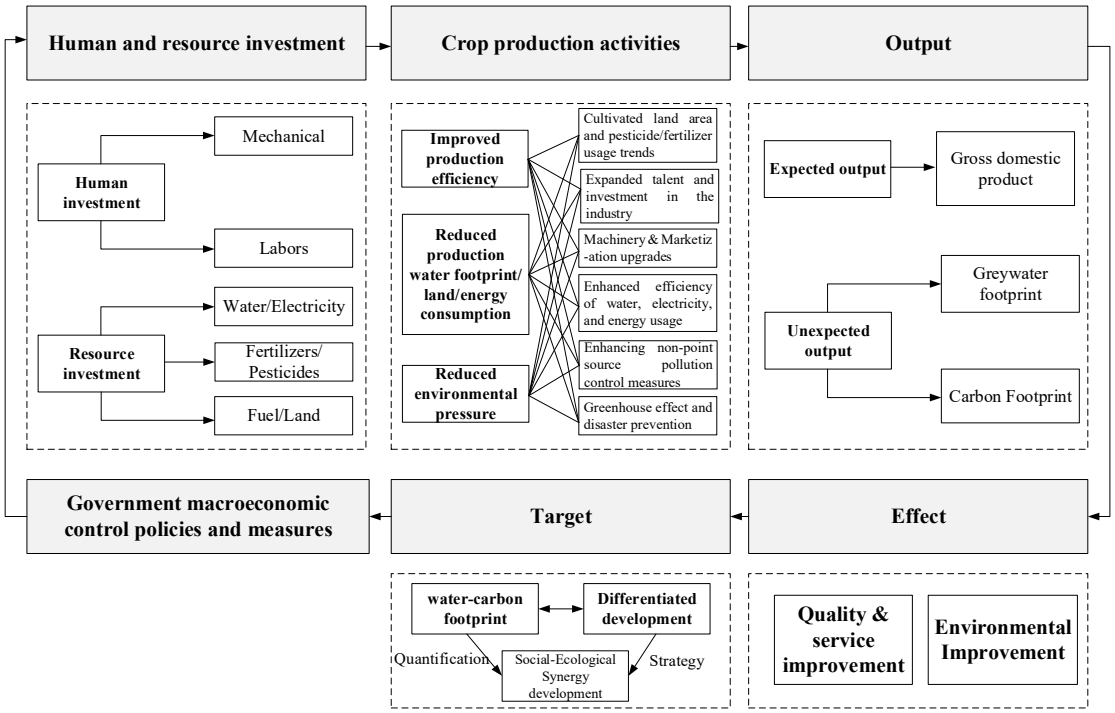

Figure 11. The correlation and driving mechanisms between industry water–carbon footprint and policy measures.

Our preliminary framework indicates that, with the continuous improvement of the market economy, both the production scale and market transaction volumes of local agricultural products have significantly increased during the study period. As the market's consumption capacity for these primary agricultural products reaches a certain level, the added value of these products tends to decrease gradually. Given that the agricultural sector has long been a pillar of economic development in the study area, it is essential, first, to segment the changes in water–carbon footprints within the crop production system into distinct phases and align these phases with the impacts of major local policies. Ultimately, this will facilitate an exploration of the coupling evolution process between agricultural water–carbon footprints and governmental policies.

Next, we conducted a mutation test and phased linear fitting analysis of the total water footprint (wf_{total}) and GHG emissions in the planting industry (Figure 12). Our findings reveal a strong correlation in the trends of water and carbon footprint changes. At a significance level of $\alpha = 0.05$, with $U(0.05) = \pm 1.96$, the points of intersection between the statistical curves of wf_{total} and GHG emissions (denoted as UBk and UFk) occurred around the years 2003 and 2005. These intersections signify the critical mutation years for both wf_{total} and GHG emissions, identified as 2003 and 2005. Dividing the study period into two distinct phases based on these mutation years reveals important insights. The results reveal a relatively stable growth trend for wf_{total} from 1990 to 2003, with an average annual increase of 3.0%. In contrast, the average annual increase rose to 4.9% from 2003 to 2015. This increase surpassed the overall average annual growth rate for the southern Xinjiang region, which was recorded at 2.7% [64]. During the period from 1990 to 2005, the GHG emissions exhibited a modest growth trend, with an average annual increase of 9.2%, which escalated to 16.2% between 2005 and 2015. These phased changes in water–carbon footprints are intricately linked to the management policies and hydraulic engineering

initiatives undertaken in the Tarim River Basin [65]. The comprehensive management plan initiated by the Chinese government in 2001 aimed to enhance local water resource allocation and management systematically. This recognition of the interplay between socio-economic development and water resource conditions has prompted active adjustments to industrial water usage structures [28]. Initially, however, local authorities relied heavily on traditional management practices, which resulted in an ambiguous approach characterized by "low water consumption, low energy consumption, and low emissions" in agriculture. This led to suboptimal management efficiency across local industries [66].

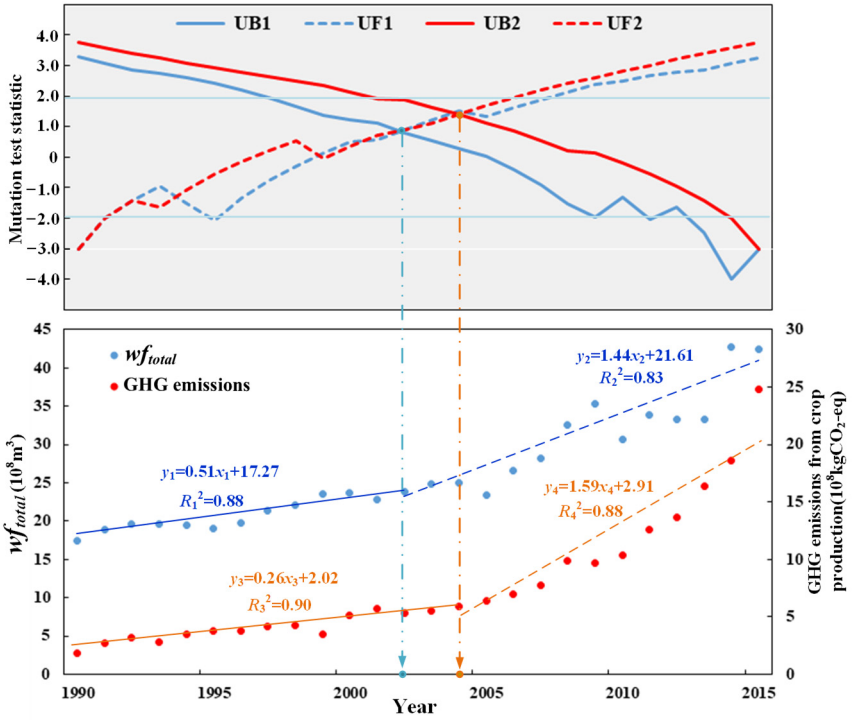

Figure 12. The mutation test and piecewise linear fitting of crop production the water–carbon footprint.

Reducing the over-reliance on the primary sector can mitigate local vulnerabilities related to water scarcity [67]. Thus, it is crucial for the government to develop diversified water usage strategies that promote greater economic efficiency in the secondary and tertiary sectors. Transitioning to an integrated water resource management framework will help balance usage patterns across sectors, ensuring a resilient water economy [68]. Moreover, policies aimed at enhancing agricultural water use efficiency, coupled with innovations in water-saving technologies within emerging productive industries, are vital for addressing the dual challenges of climate change and resource management [69]. By fostering a comprehensive understanding of the interactions between virtual water transfer, agricultural water footprints, and carbon footprints, this study provides a conceptual basis for constructing effective policy frameworks that promote sustainable development in the Yarkand River Basin and similar arid regions.

3.4.2. Discussion on Future Inter-Industry Synergistic Management Strategies

Based on our integrated pathway, combining both "top-down" and "bottom-up" methodologies, we found that the majority of local physical water and virtual water in the study area is allocated to producing low-value-added primary agricultural products. The contribution of imported virtual water to local economic production remains relatively low. The manufacturing, construction, and agricultural sectors in the study area exhibit relatively high influence and driving force correlation coefficients. These results provide a quantitative basis for optimizing industrial structures and resource management strategies. Sections 3.1 and 3.2 indicate that addressing water scarcity in the study area

primarily requires adjustments to the structure of local physical and virtual water in the primary industry. Agricultural development has long been affected by planting structures, particularly the outsized cultivation of cotton. This not only reduces yields of essential food crops, such as wheat and corn, but also negatively impacts forage production and, consequently, animal husbandry [70]. Moreover, a diversification of planting structures could enhance water resource efficiency [71]. Adjusting the cultivation of staple crops like wheat and corn may lead to better water use practices and lower carbon emissions, particularly when aligned with local climatic conditions and soil health [72]. However, external factors such as the dispersion of production units, low awareness of water conservation among farmers, and insufficient facilities have hindered the effective implementation of water-saving technologies [73]. This has resulted in little significant reduction in per-unit water consumption in the area. This situation aligns with recent studies highlighting the Jevons Paradox phenomenon in the arid regions of northwest China, which underscores the challenges of achieving efficient water use [74]. Addressing these complexities requires a holistic understanding of not only the immediate impacts of crop structure adjustments but also their long-term sustainability and potential ecological feedback mechanisms, including soil health and biodiversity enhancement [75].

The lack of effective policy incentives across counties in the study area has made it difficult for local cotton production to meet the market-oriented demands for production technology services [76]. With increasing costs for water, fertilizers, fuel, and labor, the cost of cotton production rose by nearly 50% between 2010 and 2015 [77]. In the face of intensifying market competition, there is an urgent need to accelerate resource integration and transition from a fragmented smallholder economy to an intensive management model to improve the overall resource utilization efficiency of the local "water-carbon" dominant industries. Local governments must reinforce and implement previously proposed policy measures to alleviate the current imbalance in inter-industry relationships. This includes prohibiting indiscriminate expansion of irrigation areas and land clearing, enhancing market price regulation and guaranteeing systems for major agricultural products, optimizing the proportion of "low-water-efficiency intensive" agricultural products, and introducing feasible rewards and penalties for crop farmers, as well as providing or increasing corresponding resource supply guarantees. Addressing the redistribution of virtual water in industries can strengthen the connection between local virtual water and imported virtual water by increasing the share of virtual water driven by intermediate usage in the agricultural sector. By enhancing economic and technological linkages between agriculture and other sectors, we can increase the economic added value and technical value of agricultural products, such as through the development of deep processing for agricultural products [78]. In recent years, as residents' living standards have improved, the proportion of processed agricultural and animal products in human diets has continuously risen, leading to an increasing demand for and trade volume of deep-processed agricultural products [79]. Previous quantitative studies on the water economic value of certain typical agricultural and animal products have shown that the water footprint for producing deep-processed animal products can reach 7.05 m^3/kg, which is 1.9 times that of the water footprint for primary processed cotton products [57]. Overall, while the water footprint for producing deep-processed animal products in Xinjiang is less than 13% of that for crop products, the economic value of water footprint per unit yield (measured in CNY/m^3) far exceeds that of economic crops like cotton, reaching more than five times that of cotton products. Given that the study area has relatively ample forage reserves (e.g., crop straw) [80], the local government could invest in establishing livestock breeding bases that integrate both scale and production standards through market mechanisms. Additionally, livestock waste from these breeding operations can be treated and used as organic fertilizer in local crop production, thus reducing material and energy cycles between industries, achieving goals for resource input, waste reduction, and emissions minimization [81]. This approach would enhance the utilization of local products, while

byproducts, damaged products, and waste would serve as new raw materials or resources in subsequent production cycles.

Currently, fossil fuels dominate energy production in the study area. This reliance not only leads to significant consumption of local blue water resources but also results in substantial greenhouse gas emissions, posing risks to both economic and ecological security [82]. In recent years, the government has invested in various infrastructure projects, including the construction of hydropower facilities in the upstream mountainous regions of the study area. Given that the water consumption per unit of hydropower production is significantly lower than that of traditional fossil fuels [83], and considering that water resources are a primary limiting factor for the production of resource-intensive agricultural and energy products, these projects can help alleviate issues related to resource allocation and ecological protection in downstream areas [84]. The virtual water embedded in products from the manufacturing and energy sectors can be significantly redirected into local agricultural production, thereby enhancing the economic value of virtual water within these products. As such, prioritizing the development of these sectors is recommended. With the continued implementation of policies such as those that return farmland to forests and grasslands and the "Tourism Boosting Xinjiang" strategy in the study area [85,86], the future growth of the more water- and energy-efficient secondary and tertiary industries will also provide additional employment opportunities for local residents. The government should encourage rural residents to engage in and participate in production activities that align with low-carbon and green circular development principles [87]. By establishing a virtuous cycle of economic and ecological coexistence, the unsustainable consumption of resources by local industries can be effectively reduced.

4. Conclusions

This study, focusing on the "water resources" and "greenhouse gas" emissions in the Yarkand River Basin as pivotal indicators of local resource consumption and environmental emissions, employed a suite of analytical tools, including environmental input–output modeling, CROPWAT modeling, and life cycle assessment to quantify the historical transformation patterns of physical-to-virtual water cycles within the water–carbon nexus industries. Our analysis delved into the planting industry's genuine appropriation of water resources and the associated carbon emission pressures, further elucidating the synergistic governance mechanisms that drive regional resource utilization and environmental emissions. The key findings are summarized as follows:

(1) The agricultural sector in the study area dominates the consumption of local blue and green physical water, as well as virtual water, accounting for the majority of the local water cycle flux. Demand from external markets for agricultural products from the region far exceeds local consumption, which directly increases the region's physical water use and contributes to the large outflow of blue and green virtual water. The current industrial water cycle structure in the region hinders water retention, with substantial exports of water-intensive crops, such as cotton, exacerbating local water scarcity. From the perspective of industrial linkages, it is critical to identify and prioritize industries with water retention and conservation potential. Incorporating specific industrial restructuring plans into local socio-economic development strategies will help optimize resource allocation in a more systematic and comprehensive manner.

(2) The blue and green water footprints per unit yield show a decreasing trend in the study area. However, the total crop water footprint across counties is on the rise, with annual fluctuations in the blue water footprint being more pronounced and showing greater increases compared with the green and gray water footprints. Differences in local climatic conditions, cropping patterns, irrigation practices, and economic development levels result in a spatial distribution of water footprints characterized by "higher in the mid and lower reaches, and lower in the upper reaches" of the basin. Local crop production is heavily dependent on blue water resources, making the efficient and sustainable use of these limited resources essential for promoting

the long-term development of the basin's industries. Additionally, greenhouse gas emissions from agricultural inputs and activities have shown a clear upward trend. The expansion of crop production has led to a significant increase in electricity use and the consumption of agricultural mulch, while the continued high inputs of fertilizers and agricultural mulch, along with soil N_2O emissions, are key drivers of the sharp rise in the planting industry's carbon footprint.

(3) The combination of "top-down" and "bottom-up" research pathways provides an objective and comprehensive reflection of the actual water resource consumption, transfer patterns, and GHG emissions across industries. This approach reveals the driving mechanisms behind the water–carbon footprint, shaped by industrial development and resource management policies in the basin. To ensure effective implementation of policies, local governments must address potential operational challenges. This includes adjusting the water usage structure in the primary sector and optimizing crop structures in downstream irrigation areas. A tailored approach that considers local climate conditions, market demand, and farmers' planting habits is essential. Engaging farmers in decision making and integrating climate adaptability assessments can enhance the acceptance of new practices. Accelerating resource integration and transitioning to more intensive management models are critical steps. Additionally, investing in the establishment of agricultural deep-processing industries will further enhance the economic and technical value-added of competitive products and services in the region.

Author Contributions: J.Y.: writing—original draft, review and editing, methodology, funding acquisition. S.P.: visualization, investigation, review and editing. H.C.: validation, data curation, review and editing. C.R.: software, investigation. X.L.: visualization. A.L.: supervision, formal analysis, review and editing. All authors have read and agreed to the published version of the manuscript.

Funding: This work was supported by the National Natural Science Foundation of China (Grant No. 72304245), and the "Light of West China" Program of the Chinese Academy of Sciences (Grant No. Rc924003).

Institutional Review Board Statement: Not applicable.

Informed Consent Statement: Not applicable.

Data Availability Statement: Data are contained within the article.

Acknowledgments: We also acknowledge the anonymous reviewers for helpful discussions and comments on previous manuscript versions.

Conflicts of Interest: Author Hui Cheng was employed by the company Yellow River Engineering Consulting Co., Ltd. The remaining authors declare that the research was conducted in the absence of any commercial or financial relationships that could be construed as a potential conflict of interest.

Appendix A

Table A1. Reclassification and consolidation of economic industrial system sectors.

Code	42 Sectors in the Original IO table	Aggregated 28 Sectors	Code	42 Sectors in the Original IO Table	Aggregated 28 Sectors
1	Planting sectors, forestry, animal husbandry and fishery	Agriculture (D1)	23	Electricity and heat production and supply	Electricity and heat production and supply (D22)
2	Coal mining and washing	Coal mining and washing (D2)	24	Gas production and supply	Gas and water production and supply (D23)
3	Oil and gas extraction	Oil and gas extraction (D3)	25	Water production and supply industry	
4	Metal mining and dressing	Metal mining and dressing (D4)	26	Construction	Construction (D24)

Table A1. *Cont.*

Code	42 Sectors in the Original IO table	Aggregated 28 Sectors	Code	42 Sectors in the Original IO Table	Aggregated 28 Sectors
5	Non-metallic minerals and other minerals mining and dressing	Non-metallic minerals mining and dressing (D5)	27	Transportation and warehousing	Transportation, warehousing and postal services (D25)
6	Food manufacturing and tobacco processing	Food manufacturing and processing (D6)	28	Postal industry	
7	Textile industry	Textile industry (D7)	29	Information transmission, computer services and software industry	
8	Textile clothing, shoes, hats, leather, down and their products industry	Clothing, leather, down and their products industry (D8)	30	Wholesale and retail industry	Wholesale and retail trade industry (D26)
9	Wood processing and furniture manufacturing industry	Wood processing manufacturing industry (D9)	31	Accommodation and catering industry	Accommodation and catering industry (D27)
10	Papermaking, printing and cultural and educational sports goods manufacturing industry	Papermaking, printing and cultural and educational goods manufacturing industry (D10)	32	Financial industry	
11	Petroleum processing, coking and nuclear fuel processing industry	Petroleum processing, coking and nuclear fuel processing industry (D11)	33	Real estate industry	Other service industries (D28)
12	Chemical industry	Chemical industry (D12)	34	Leasing and business services industry	
13	Non-metallic mineral products industry	Non-metallic mineral products (D13)	35	Research and development	
14	Metal smelting and rolling processing	Metal smelting and rolling processing (D14)	36	Comprehensive technical services	
15	Metal products	Metal products (D15)	37	Water conservancy, environment and public facilities management	
16	General and special equipment manufacturing	General and special equipment manufacturing (D16)	38	Residential services and other services	
17	Transportation equipment manufacturing	Transportation equipment manufacturing (D17)	39	Education	
18	Electrical machinery and equipment manufacturing	Electrical, machinery and equipment manufacturing (D18)	40	Health, social security and social welfare	
19	Communication equipment, computer and other electronic equipment manufacturing	Communication, computer and other electronic equipment manufacturing (D19)	41	Culture, sports and entertainment	
20	Instruments and cultural office machinery manufacturing	Instruments and cultural office machinery manufacturing (D20)	42	Public administration and social organizations	
21	Handicrafts and other manufacturing	Other industries (D21)			
22	Waste and scrap				

Appendix B

The matrix C for the total consumption of local and imported goods by economic sectors is given by the following:

$$C = k + h = \left[(I - A)^{-1} - I \right] \cdot \hat{y} \tag{A1}$$

where C is the total consumption matrix for local and imported goods by economic sectors and $\hat{y}$ represents the diagonal matrix.

The total consumption matrix for local goods (C^k) and imported goods (C^h) during the production process is expressed as follows:

$$C^k = C - C^h = C - \hat{k} \cdot \left(\hat{k} + \hat{h} \right)^{-1} \cdot C \tag{A2}$$

where $\hat{k}$ and $\hat{h}$ are the diagonal matrices of the total intermediate use of local and imported goods, respectively.

The virtual water coefficient matrix for the economic sectors, from the production perspective, is given by the following:

$$w^t = w^d \cdot (I - A)^{-1} \tag{A3}$$

where w^t represents the total water consumption coefficient matrix and w^d represents the direct water consumption coefficient matrix.

Thus, the matrix for the transfer of local physical water in the economic sectors' production process (W^k) can be expressed as follows:

$$W^k = \hat{w}^d \cdot C^k \tag{A4}$$

The substitution method is widely used in regional energy trade research [88]. It is also applied here to calculate the virtual water embodied in imported goods. The transfer matrix of imported virtual water during economic production (W^h) is represented as follows:

$$W^h = \hat{w}^t \cdot C^h \tag{A5}$$

In the extended input–output analysis for water resources, the reallocation of both local water consumption and imported virtual water among sectors is expressed as follows:

$$V = \hat{w}^t \cdot (f_1 + f_2 + e) \tag{A6}$$

References

1. Gomiero, T. Soil degradation, land scarcity and food security: Reviewing a complex challenge. *Sustainability* **2016**, *8*, 281. [CrossRef]
2. Scanlon, B.R.; Fakhreddine, S.; Rateb, A.; Graaf, I.; Famiglietti, J.; Gleeson, T.; Grafton, R.Q.; Jobbagy, E.; Kebede, S.; Kolusu, S.R.; et al. Global water resources and the role of groundwater in a resilient water future. *Nat. Rev. Earth Environ.* **2023**, *4*, 87–101. [CrossRef]
3. Haddeland, I.; Heinke, J.; Biemans, H.; Eisner, S.; Flörke, M.; Hanasaki, N.; Konzmann, M.; Ludwig, F.; Masaki, Y.; Schewe, J.; et al. Global water resources affected by human interventions and climate change. *Proc. Natl. Acad. Sci. USA* **2014**, *111*, 3251–3256. [CrossRef] [PubMed]
4. Liu, Y.; Chen, B.; Wei, W.; Shao, L.; Li, Z.; Jiang, W.; Chen, G. Global water use associated with energy supply, demand and international trade of China. *Appl. Energy* **2020**, *257*, 113992. [CrossRef]
5. Bilgen, S. Structure and environmental impact of global energy consumption. *Renew. Sustain. Energy Rev.* **2014**, *38*, 890–902. [CrossRef]
6. Wang, S.; Fu, B.; Bodin, Ö.; Liu, J.; Zhang, M.; Li, X. Alignment of social and ecological structures increased the ability of river management. *Sci. Bull.* **2019**, *64*, 1318–1324. [CrossRef]
7. Patterson, M.; McDonald, G.; Hardy, D. Is there more in common than we think? Convergence of ecological footprinting, emergy analysis, life cycle assessment and other methods of environmental accounting. *Ecol. Model.* **2017**, *362*, 19–36. [CrossRef]

8. Yu, H. A review of input–output models on multisectoral modelling of transportation–economic linkages. *Transp. Rev.* **2018**, *38*, 654–677. [CrossRef]
9. Zhao, L.; Sun, C.; Liu, F. Interprovincial two-stage water resource utilization efficiency under environmental constraint and spatial spillover effects in China. *J. Clean. Prod.* **2017**, *164*, 715–725. [CrossRef]
10. Sun, X.; Li, J.; Qiao, H.; Zhang, B. Energy implications of China's regional development: New insights from multi-regional input-output analysis. *Appl. Energy* **2017**, *196*, 118–131. [CrossRef]
11. Bachmann, C.; Roorda, M.J.; Kennedy, C. Developing a multi-scale multi-region input–output model. *Econ. Syst. Res.* **2015**, *27*, 172–193. [CrossRef]
12. He, P.; Ng, T.S.; Su, B. Energy-economic resilience with multi-region input–output linear programming models. *Energy Econ.* **2019**, *84*, 104569. [CrossRef]
13. Matuštík, J.; Kočí, V. What is a footprint? A conceptual analysis of environmental footprint indicators. *J. Clean. Prod.* **2021**, *285*, 124833. [CrossRef]
14. Hogeboom, R.J. The water footprint concept and water's grand environmental challenges. *One Earth* **2020**, *2*, 218–222. [CrossRef]
15. Steinmann, Z.J.N.; Schipper, A.M.; Hauck, M.; Huijbregts, M.A.J. How many environmental impact indicators are needed in the evaluation of product life cycles? *Environ. Sci. Technol.* **2016**, *50*, 3913–3919. [CrossRef]
16. Mekonnen, M.M.; Romanelli, T.L.; Ray, C.; Hoekstra, A.Y.; Liska, A.J.; Neale, C.M.U. Water, Energy, and Carbon Footprints of Bioethanol from the US and Brazil. *Environ. Sci. Technol.* **2018**, *52*, 14508–14518; Erratum in *Environ. Sci. Technol.* **2020**, *54*, 7734. [CrossRef]
17. Mekonnen, M.M.; Gerbens-Leenes, W. The water footprint of global food production. *Water* **2020**, *12*, 2696. [CrossRef]
18. Rondoni, A.; Grasso, S. Consumers behaviour towards carbon footprint labels on food: A review of the literature and discussion of industry implications. *J. Clean. Prod.* **2021**, *301*, 127031. [CrossRef]
19. Gu, Y.; Wang, H.; Robinson, Z.P.; Wang, X.; Wu, J.; Li, Y.; Xu, J.; Li, F. Environmental footprint assessment of green campus from a food-water-energy nexus perspective. *Energy Procedia* **2018**, *152*, 240–246. [CrossRef]
20. Karwacka, M.; Ciurzyńska, A.; Lenart, A.; Janowicz, M. Sustainable development in the agri-food sector in terms of the carbon footprint: A Review. *Sustainability* **2020**, *12*, 6463. [CrossRef]
21. Hou, Y.; Chen, Y.; Ding, J.; Li, Z.; Li, Y.; Sun, F. Ecological impacts of land use change in the arid Tarim River Basin of China. *Remote Sens.* **2022**, *14*, 1894. [CrossRef]
22. Delbourg, E.; Dinar, S. The globalization of virtual water flows: Explaining trade patterns of a scarce resource. *World Dev.* **2020**, *131*, 104917. [CrossRef]
23. Liu, X.; Liu, W.; Tang, Q.; Liu, B.; Wada, Y.; Yang, H. Global agricultural water scarcity assessment incorporating blue and green water availability under future climate change. *Earth's Future* **2022**, *10*, e2021EF002567. [CrossRef]
24. Gao, D.; Long, A.; Yu, J.; Xu, H.; Su, S.; Zhao, X. Assessment of inter-sectoral virtual water reallocation and linkages in the Northern Tianshan Mountains, China. *Water* **2020**, *12*, 2363. [CrossRef]
25. Yu, J.; Long, A.; Lai, X.; Elbeltagi, A.; Deng, X.; Gu, X.; Heng, T.; Cheng, H.; Oel, P.V. Evaluating sustainable intensification levels of dryland agriculture: A focus on Xinjiang, China. *Ecol. Indic.* **2024**, *158*, 111448. [CrossRef]
26. Sun, F.; Wang, Y.; Chen, Y.; Li, Y.; Zhang, Q.; Qin, J.; Kayumba, P.M. Historic and simulated desert-oasis ecotone changes in the arid Tarim River Basin, China. *Remote Sens.* **2021**, *13*, 647. [CrossRef]
27. Guo, J.; Xu, H.; Zhang, G.; Yuan, K.; Ling, H. The enhanced management of water resources improves ecosystem services in a typical arid basin. *Sustainability* **2020**, *12*, 8802. [CrossRef]
28. Li, W.; Huang, F.; Shi, F.; Wei, X.; Zamanian, K.; Zhao, X. Human and climatic drivers of land and water use from 1997 to 2019 in Tarim River basin, China. *Int. Soil Water Conserv. Res.* **2021**, *9*, 532–543. [CrossRef]
29. Zhang, M.; Huang, X. Effects of industrial restructuring on carbon reduction: An analysis of Jiangsu Province, China. *Energy* **2012**, *44*, 515–526. [CrossRef]
30. Wang, Y.; Xiao, H.; Lu, M.F. Analysis of water consumption using a regional input-output model: Model development and application to Zhangye City, Northwestern China. *J. Arid Environ.* **2009**, *73*, 894–900. [CrossRef]
31. Deng, G.; Ma, Y.; Li, X. Regional water footprint evaluation and trend analysis of China-Based on interregional input-output model. *J. Clean. Prod.* **2016**, *112*, 4674–4682. [CrossRef]
32. Allegretti, G.; Montoya, M.A.; Talamini, E. Assessing sectoral water stress states from the demand-side perspective through water footprint dimensions decomposition. *Sci. Total Environ.* **2022**, *809*, 152216. [CrossRef]
33. Zhong, M.; Shoujuan, S.; Aihua, L.; Xiaoxia, Z. Water cycle analysis of social and economic system in Tarim River Basin. *Adv. Earth Sci.* **2018**, *33*, 833. (In Chinese)
34. Yin, J.; Wang, H.; Cai, Y. Water footprint calculation on the basis of input-output analysis and a biproportional algorithm: A case study for the Yellow River Basin, China. *Water* **2016**, *8*, 363. [CrossRef]
35. Hou, R.; Li, S.; Chen, H.; Ren, G.; Gao, W.; Liu, L. Coupling mechanism and development prospect of innovative ecosystem of clean energy in smart agriculture based on blockchain. *J. Clean. Prod.* **2021**, *319*, 128466. [CrossRef]
36. Rosa, L.; Chiarelli, D.D.; Tu, C.; Rulli, M.C.; D'Odorico, P. Global unsustainable virtual water flows in agricultural trade. *Environ. Res. Lett.* **2019**, *14*, 114001. [CrossRef]
37. Wichelns, D. Virtual water and water footprints do not provide helpful insight regarding international trade or water scarcity. *Ecol. Indic.* **2015**, *52*, 277–283. [CrossRef]

38. Zhang, Y.; Zhang, J.; Tang, G.; Chen, M.; Wang, L. Virtual water flows in the international trade of agricultural products of China. *Sci. Total Environ.* **2016**, *557*, 1–11. [CrossRef]
39. Long, A.; Yu, J.; He, X.; Deng, X.; Su, S.; Zhang, J.; Ren, C.; Zhang, P.; Hai, Y. Linking local water consumption in inland arid regions with imported virtual water: Approaches, application and actuators. *Adv. Water Resour.* **2021**, *151*, 103906. [CrossRef]
40. Li, X.; Cheng, G.; Ge, Y.; Li, H.; Han, F.; Hu, X.; Tian, W.; Tian, Y.; Pan, X.; Nian, Y.; et al. Hydrological cycle in the Heihe River Basin and its implication for water resource management in endorheic basins. *J. Geophys. Res. Atmos.* **2018**, *123*, 890–914. [CrossRef]
41. Cao, L.; Wu, P.; Zhao, X.; Wang, Y. Evaluation of grey water footprint of grain production in Hetao Irrigation District, Inner Moreongolia. *Trans. Chin. Soc. Agric. Eng.* **2014**, *30*, 63–72. (In Chinese)
42. Zhang, T.; Zhai, Y.; Ma, X.; Shen, X.; Bai, Y.; Zhang, R.; Ji, C.; Hong, J. Towards environmental sustainability: Life cycle assessment-based water footprint analysis on China's cotton production. *J. Clean. Prod.* **2021**, *313*, 127925. [CrossRef]
43. Feng, M.; Chen, Y.; Duan, W.; Zhu, Z.; Wang, C.; Hu, Y. Water-energy-carbon emissions nexus analysis of crop production in the Tarim river basin, Northwest China. *J. Clean. Prod.* **2023**, *396*, 136566. [CrossRef]
44. Hu, L.; Wen, L.; Peng, Y.; Yi, Q.; Xu, L. Evaluation of production and carbon benefit of different vegetables. *J. Agric. Resour. Environ.* **2016**, *33*, 92–101. (In Chinese)
45. Liu, S.; Wang, X.; Hu, J.; Li, Q.; Cui, L.; Duan, X.; Guo, L. Effects of fertilization and irrigation on the carbon footprint of alfalfa in Gansu Province. *Sci. Agric. Sin.* **2018**, *51*, 556–565.
46. Walling, E.; Vaneeckhaute, C. Greenhouse gas emissions from inorganic and organic fertilizer production and use: A review of emission factors and their variability. *J. Environ. Manag.* **2020**, *276*, 111211. (In Chinese) [CrossRef]
47. Ma, R.; Zou, J.; Han, Z.; Yu, K.; Wu, S.; Li, Z.; Liu, S.; Niu, S.; Horwath, W.R.; Zhu-Barker, X. Global soil-derived ammonia emissions from agricultural nitrogen fertilizer application: A refinement based on regional and crop-specific emission factors. *Glob. Chang. Biol.* **2021**, *27*, 855–867. [CrossRef]
48. Li, N.; Shang, L.; Yu, Z.; Jiang, Y. Estimation of agricultural greenhouse gases emission in interprovincial regions of China during 1996–2014. *Nat. Hazards* **2020**, *100*, 1037–1058. [CrossRef]
49. Xiong, C.; Yang, D.; Xia, F.; Huo, J. Changes in agricultural carbon emissions and factors that influence agricultural carbon emissions based on different stages in Xinjiang, China. *Sci. Rep.* **2016**, *6*, 36912. [CrossRef]
50. Günther, J.; Thevs, N.; Gusovius, H.J.; Sigmund, I.; Brückner, T.; Beckmann, V.; Abdusalik, N. Carbon and phosphorus footprint of the cotton production in Xinjiang, China, in comparison to an alternative fibre (Apocynum) from Central Asia. *J. Clean. Prod.* **2017**, *148*, 490–497. [CrossRef]
51. Long, A.; Zhang, P.; Hai, Y.; Deng, X.; Li, J.; Wang, J. Spatio-temporal variations of crop water footprint and its influencing factors in Xinjiang, China during 1988–2017. *Sustainability* **2020**, *12*, 9678. [CrossRef]
52. Ren, C.; Zhang, P.; Deng, X.; Zhang, J.; Wang, Y.; Wang, S.; Yu, J.; Lai, X.; Long, A. Unveiling the dynamics and influence of water footprints in arid areas: A case study of Xinjiang, China. *Water* **2024**, *16*, 1164. [CrossRef]
53. Hai, Y.; Long, A.; Zhang, P.; Deng, X.; Li, J.; Deng, M. Evaluating agricultural water-use efficiency based on water footprint of crop values: A case study in Xinjiang of China. *J. Arid Land* **2020**, *12*, 580–593. [CrossRef]
54. Li, Y.; Deng, M. Spatiotemporal variations of agricultural water footprint and its economic benefits in Xinjiang, northwestern China. *Sci. Rep.* **2021**, *11*, 23864. [CrossRef]
55. Huang, S.; Wortmann, M.; Duethmann, D.; Menz, C.; Shi, F.; Zhao, C.; Su, B.; Krysanova, V. Adaptation strategies of agriculture and water management to climate change in the Upper Tarim River basin, NW China. *Agric. Water Manag.* **2018**, *203*, 207–224.
56. Chen, Y.; Zhang, X.; Fang, G.; Li, Z.; Wang, F.; Qin, J.; Sun, F. Potential risks and challenges of climate change in the arid region of northwestern China. *Reg. Sustain.* **2020**, *1*, 20–30.
57. Zhang, P.; Deng, X.; Long, A.; Hai, Y.; Wang, H.; Xu, H. Impact of social factors in agricultural production on the crop water footprint in Xinjiang, China. *Water* **2018**, *10*, 1145. [CrossRef]
58. Wu, P.; Sun, S.; Wang, Y.; Li, X.; Zhao, X. Research on the quantification methods for water footprint of crop production. *J. Hydraul. Eng.* **2017**, *48*, 651–660+669. (In Chinese)
59. Cao, X.; Ren, J.; Wu, M.; Guo, X.; Wang, W. Assessing agricultural water use effect of China based on water footprint framework. *Trans. Chin. Soc. Agric. Eng.* **2018**, *34*, 1–8. (In Chinese)
60. Xu, S.; He, W.; Yuan, L.; Degefu, D.M.; Yang, Y.; Li, H. The relationship between coordination degree of the water–energy–food system and regional economic development. *Sustainability* **2021**, *13*, 1305. [CrossRef]
61. Song, T.; Liu, W.; Liu, Z.; Wuzhati, Y. Policy mobilities and the China model: Pairing aid policy in Xinjiang. *Sustainability* **2019**, *11*, 3496. [CrossRef]
62. Xiong, Y.; Zhang, Q.; Chen, X.; Bao, M.; Zhang, J.; Wang, Y. Large scale agricultural plastic mulch detecting and monitoring with multi-source remote sensing data: A case study in Xinjiang, China. *Remote Sens.* **2019**, *11*, 2088. [CrossRef]
63. Zhou, X.; Yu, J.; Li, J.; Zhang, D.; Wu, D.; Pan, S.; Chen, W. Spatial correlation among cultivated land intensive use and carbon emission efficiency: A case study in the Yellow River Basin, China. *Environ. Sci. Pollut. Res.* **2022**, *29*, 43341–43360. [CrossRef] [PubMed]
64. Zhang, P.; Deng, M.; Long, A.; Deng, X.; Wang, H.; Hai, Y.; Wang, J.; Liu, Y. Coupling analysis of social-economic water consumption and its effects on the arid environments in Xinjiang of China based on the water and ecological footprints. *J. Arid Land* **2020**, *12*, 73–89. [CrossRef]

65. Zuo, Q.; Zhao, H.; Mao, C.; Ma, J.; Cui, G. Quantitative analysis of human-water relationships and harmony-based regulation in the Tarim River Basin. *J. Hydrol. Eng.* **2015**, *20*, 05014030. [CrossRef]
66. Feng, M.; Chen, Y.; Duan, W.; Fang, G.; Li, Z.; Jiao, L.; Sun, F.; Li, Y.; Hou, Y. Comprehensive evaluation of the water-energy-food nexus in the agricultural management of the Tarim River Basin, Northwest China. *Agric. Water Manag.* **2022**, *271*, 107811. [CrossRef]
67. Adeyeye, K.; Gibberd, J.; Chakwizira, J. Water marginality in rural and peri-urban communities. *J. Clean. Prod.* **2020**, *273*, 122594. [CrossRef]
68. Falkenmark, M.; Wang-Erlandsson, L.; Rockström, J. Understanding of water resilience in the Anthropocene. *J. Hydrol. X* **2019**, *2*, 100009. [CrossRef]
69. Lakhiar, I.A.; Yan, H.; Zhang, C.; Wang, G.; He, B.; Hao, B.; Han, Y.; Wang, B.; Bao, R.; Syed, T.N.; et al. A Review of Precision Irrigation Water-Saving Technology under Changing Climate for Enhancing Water Use Efficiency, Crop Yield, and Environmental Footprints. *Agriculture* **2024**, *14*, 1141. [CrossRef]
70. Wang, F.; Chen, Y.; Li, Z.; Fang, J.; Li, Y.; Xia, Z. Assessment of the irrigation water requirement and water supply risk in the Tarim River Basin, Northwest China. *Sustainability* **2019**, *11*, 4941. [CrossRef]
71. Hatfield, J.L.; Dold, C. Water-use efficiency: Advances and challenges in a changing climate. *Front. Plant Sci.* **2019**, *10*, 103. [CrossRef] [PubMed]
72. Chen, X.; Ma, C.; Zhou, H.; Liu, Y.; Huang, X.; Wang, M.; Cai, Y.; Su, D.; Muneer, M.A.; Guo, M.; et al. Identifying the main crops and key factors determining the carbon footprint of crop production in China, 2001–2018. *Resour. Conserv. Recycl.* **2021**, *172*, 105661. [CrossRef]
73. Ju, H.; Liu, Y.; Zhang, S. Interprovincial agricultural water footprint in China: Spatial pattern, driving forces and implications for water resource management. *Sustain. Prod. Consum.* **2023**, *43*, 264–277. [CrossRef]
74. Wang, Y.; Long, A.; Xiang, L.; Deng, X.; Zhang, P.; Hai, Y.; Wang, J.; Li, Y. The verification of Jevons' paradox of agricultural water conservation in Tianshan District of China based on water footprint. *Agric. Water Manag.* **2020**, *239*, 106163. [CrossRef]
75. Tahat, M.M.; Alananbeh, K.M.; Othman, Y.A.; Leskovar, D.I. Soil health and sustainable agriculture. *Sustainability* **2020**, *12*, 4859. [CrossRef]
76. Zhang, J.; Mishra, A.K.; Hirsch, S. Market-oriented agriculture and farm performance: Evidence from rural China. *Food Policy* **2021**, *100*, 102023. [CrossRef]
77. Cheng, W.; Wang, L. How to reduce the cost of cotton cultivation? A Case Study of Xinjiang, China. *Custos E Agronegocio Line* **2019**, *15*, 458–470.
78. De Roest, K.; Ferrari, P.; Knickel, K. Specialisation and economies of scale or diversification and economies of scope? Assessing different agricultural development pathways. *J. Rural Stud.* **2018**, *59*, 222–231. [CrossRef]
79. Li, T. Problems and Countermeasures of China's International Trade in Agricultural Products under the "Belt and Road Initiative". *Sci. Program.* **2022**, *2022*, 5093426. [CrossRef]
80. Wang, G.; Li, Y.; Fan, L.; Ma, X.; Liang, Y.; Hui, T.; Zhang, W.; Li, W.; Mao, J. Assessment of grassland carrying capacity drivers and evaluation of pasture-livestock balance: A case study of Xinjiang, China. *Glob. Ecol. Conserv.* **2024**, *55*, e03203. [CrossRef]
81. Yang, G.; Li, J.; Liu, Z.; Zhang, Y.; Xu, X.; Zhang, H.; Xu, Y. Research trends in crop–livestock systems: A bibliometric review. *Int. J. Environ. Res. Public Health* **2022**, *19*, 8563. [CrossRef] [PubMed]
82. Cui, C.; Shan, Y.; Liu, J.; Yu, X.; Wang, H.; Wang, Z. CO_2 emissions and their spatial patterns of Xinjiang cities in China. *Appl. Energy* **2019**, *252*, 113473. [CrossRef]
83. Zou, C.; Zhao, Q.; Zhang, G.; Xiong, B. Energy revolution: From a fossil energy era to a new energy era. *Nat. Gas Ind. B* **2016**, *3*, 1–11. [CrossRef]
84. Li, Y.; Zhang, L.; Zhang, P.; Li, X.; Hao, Y. Water-energy-food nexus in China: An interregional comparison. *Agric. Water Manag.* **2024**, *301*, 108964. [CrossRef]
85. Wang, Y.; Li, C.; Ochege, F.U.; Han, Q.; Hellwich, O.; Wu, S.; Luo, G. Contribution of cropland expansion to regional carbon stocks in an arid area of China: A case study in Xinjiang. *Carbon Manag.* **2022**, *13*, 42–54. [CrossRef]
86. Wu, Y.; Wang, Y. An empirical study on the tourist cognitive evaluations of tourism public services in Xinjiang province, China. *Sustainability* **2024**, *16*, 1712. [CrossRef]
87. Xiao, L.; Xinping, L.; Zhenbo, L. Coupling of ecological economic system in Tarim River Watershed. In *Ecological Economics and Harmonious Society*; Springer: Singapore, 2016; pp. 197–208.
88. Ying, C.; Jiahua, P.; Laihui, X. Energy embodied in goods in international trade of China: Calculation and policy implications. *Chin. J. Popul. Resour. Environ.* **2011**, *9*, 16–32. (In Chinese) [CrossRef]

Disclaimer/Publisher's Note: The statements, opinions and data contained in all publications are solely those of the individual author(s) and contributor(s) and not of MDPI and/or the editor(s). MDPI and/or the editor(s) disclaim responsibility for any injury to people or property resulting from any ideas, methods, instructions or products referred to in the content.